SILVER NANOWIRE/CHITOSAN NANOCOMPOSITE DRY ELECTRODES FOR ELECTROCARDIOGRAM

A THESIS SUBMITTED TO
THE GRADUATE SCHOOL OF NATURAL AND APPLIED SCIENCES
OF
MIDDLE EAST TECHNICAL UNIVERSITY

BY

SÜLEYMAN KAZIM SÖMEK

IN PARTIAL FULFILLMENT OF THE REQUIREMENTS
FOR
THE DEGREE OF MASTER OF SCIENCE
IN
MICRO AND NANOTECHNOLOGY

DECEMBER 2019

Approval of the thesis:

SILVER NANOWIRE/CHITOSAN NANOCOMPOSITE DRY ELECTRODES FOR ELECTROCARDIOGRAM

submitted by **SÜLEYMAN KAZIM SÖMEK** in partial fulfillment of the requirements for the degree of **Master of Science in Micro and Nanotechnology Department, Middle East Technical University** by,

Prof. Dr. Halil Kalıpçılar
Dean, Graduate School of **Natural and Applied Sciences** _____

Prof. Dr. Almıla Güvenç Yazıcıoğlu
Head of Department, **Micro and Nanotechnology** _____

Prof. Dr. Hüsnü Emrah Ünalan
Supervisor, **Micro and Nanotechnology, METU** _____

Prof. Dr. Derek K. Baker
Co-Supervisor, **Mechanical Engineering Dept., METU** _____

Examining Committee Members:

Prof. Dr. Ali Çırpan
Chemistry, METU _____

Prof. Dr. Hüsnü Emrah Ünalan
Micro and Nanotechnology, METU _____

Assoc. Prof. Dr. Eda Ayşe Aksoy
Basic Pharmaceutical Science Department, Hacettepe Uni., _____

Assist. Prof. Dr. Simge Çınar
Metallurgical and Materials Enginering Dept. METU _____

Assoc. Prof. Dr. Yeşim Serinağaoğlu
Electrical and Electronic Engineering. METU _____

Date: 10.12.2019

I hereby declare that all information in this document has been obtained and presented in accordance with academic rules and ethical conduct. I also declare that, as required by these rules and conduct, I have fully cited and referenced all material and results that are not original to this work.

Name, Surname: Süleyman Kazım Sömek

Signature:

ABSTRACT

SILVER NANOWIRE/CHITOSAN NANOCOMPOSITE DRY ELECTRODES FOR ELECTROCARDIOGRAM

Sömek, Süleyman Kazım
Master of Science, Micro and Nanotechnology
Supervisor: Prof. Dr. Hüsnü Emrah Ünalan
Co-Supervisor: Prof. Dr. Derek K. Baker

December 2019, 58 pages

Nanocomposites of chitosan and silver nanowires (Ag NWs) were fabricated and their mechanical, thermal, electrical and antibacterial properties were investigated. A simple solvent casting method was used for the fabrication of nanocomposites with different Ag NW loadings ranging from 1 wt.% to 40 wt.%. Nanowires showed excellent dispersion in chitosan matrix. Antibacterial properties of the Ag NW/ chitosan nanocomposites were investigated against different bacteria strains of American type culture Collection (ATCC) using conventional microbiological methods. Prepared nanocomposites were found to have high antibacterial affect against Staphylococcus aureus, (ATCC #25923), Escherichia coli (ATCC#25922), Bacillus cereus (ATCC#14603) and Candida albicans (ATCC #90028) strains. Following the demonstration of antibacterial activity, fabricated nanocomposites were used as in-vitro electrocardiogram (ECG) electrodes. ECG measurement results showed that higher nanowire loadings within the nanocomposites have better performance in terms of recording useful ECG signals. Results presented herein showed that the Ag NW/ chitosan nanocomposites have a very high potential to be used as dry electrodes for ECG and offers simple and easy fabrication.

Keywords: Chitosan Ag NW, ECG Electrode, Electrical Characterization, Thermal Characterization, Antibacterial Performance

ÖZ

ELEKTROKARDIYOGRAM IÇIN GÜMÜŞ NANOTEL / KITOSAN NANOKOMPOZIT KURU ELEKTROTLAR

Sömek, Süleyman Kazım
Yüksek Lisans, Mikro ve Nanoteknoloji
Tez Danışmanı: Prof. Dr. Hüsnü Emrah Ünalan
Ortak Tez Danışmanı: Prof. Dr. Derek K. Baker

Aralık 2019, 58 sayfa

Bu tez çalışmasında, kitosan biyo-polimer ve gümüş nanotel kombine biyo-polimer kompozit malzemenin imalatı ve termal ve elektriksel karakterizasyonu incelenmiştir. Kitosan Gümüş Nanoteller, solvent döküm metoduyla üretilmiştir. Elektrokardiyogram için Gümüş Nanotel / Kitosan Nanokompozit Kuru Elektrotlar Nanokompozitlerin imalatında, ağırlıkça %1-40 arasında değişen gümüş nanotel yüklemesi için basit bir "solvent casting" yöntemi kullanılmıştır. Nanoteller kitosan matrisinde mükemmel dağılım göstermiştir. Ag NW / chitosan nanokompozitlerin antibakteriyel özellikleri, geleneksel mikrobiyolojik yöntemler kullanılarak Amerikan tipi kültür Koleksiyonunun (ATCC)*Staphylococcus aureus*, (ATCC # 25923), *Escherichia coli* (ATCC # 25922), *Bacillus cereus* (ATCC # 14603) ve Candida albicans (ATCC # 90028) bakteri suşlarına karşı araştırılmıştır.Hazırlanan nanokompozitlerin, antibakteriyel etkisinin yüksek olduğu tespit edilmiştir. Son olarak üretilen nanokompozitler, in vitro ECG elektrotları olarak kullanılmıştır. EKG ölçüm sonuçları, ağırlıkça% artan nanokompozitlerin faydalı EKG sinyallerinin kaydedilmesi bakımından daha iyi performansa sahip olduğunu göstermektedir.

Anahtar Kelimeler: Gümüş Nanotel, Kitosan, Biyonanokompozit, Karakterizasyon , Malzeme iyiliştirme

To my Family…

ACKNOWLEDGEMENTS

First of all, I would like to express my deepest gratitude to my supervisor Prof. Dr. Hüsnü Emrah Ünalan for his continuous support, guidance, patience, motivation, from the very beginning of this thesis study. Without Nanomaterials and Devices Laboratory facilities this study will never be completed. Also, I thank very much to my co-advisor Prof. Dr. Derek K. Baker for his valuable support, knowledge, engineering approach and mentoring since my undergraduate years.

I am deeply grateful to Assoc. Prof. Dr. Gülçin Akça and her group members, our collaborators in Gazi University for their unlimited assistance, technical contribution, insightful comments and positive approach. Antibacterial performance evaluation study has been done by their group and necessary standard equipment and standard bacteria culture have been generously provided by them.

I would like to thank Assoc. Prof. Dr. Yeşim Serinağaoğlu for her valuable support and Kardinero Medikal A.Ş for their support on ECG recordings. They have provided the ECG device and ECG measurements have been conducted with their operators. Also, I would like to thank Doğa Doğanay and Assist. Prof. Dr. Şahin Coşkun for their guidance, who are my mentors in this thesis.

Also, I would like to thank to my father Remzi Sömek and my mother Ümmühan Sömek for their patience and support during my thesis study. Finally, I am deeply gratefull to my wife Betül Sömek for her support during my thesis.

TABLE OF CONTENTS

LIST OF TABLES

TABLES

LIST OF FIGURES

FIGURES

LIST OF ABBREVIATIONS

$AgNO_3$: Silver nitrate

Ag NP: Silver nanoparticle

Ag NW: Silver nanowire

B. cereous: Bacillus cereus

C.albicans: Candida albicans

CNT: Carbon nano tube

CPE: Conductive polymer electrode

DSC: Differential scanning calorimetry

E. coli: Escherichia coli

EG: Ethylene glycol

FTIR: Foruer Transform Infrared Spectroscopy

LA: Lactic acid

NaCl: Sodium chloride

PDMS: Polydimethylsiloxane

PLA: Polylactic Acid

S.aureus: Staphylococcus aureus

SEM: Scanning electron microscopy

TGA: Thermo gravimetric analysis

CHAPTER 1

INTRODUCTION

Wearable technologies, especially in the field of health care, have received great deal of attention in recent years with the emerging devices in this field. They are intended to be used in daily life in a variety of ways due to the potential to detect sudden changes in health status and allow early intervention.

One of the most critical disorders in sudden health status changes and fatal cases is heart disease. Heart attacks and similar abnormal heart conditions must be monitored continuously and recognized beforehand. Electrocardiogram (ECG) measures body polarization. Continuous monitoring of the heart is possible by making ECG suitable for wearable technology. It is crucial for a wearable ECG electrode to be compatible with the elastic body instead of being a solid metal and better to exhibit antimicrobial properties since it will be in constant contact with the tissue.

Long-term ECG measurements are sought after for early diagnostics of cardiac diseases. Conventional silver/silver chloride (Ag/AgCl) electrodes makes use of an electrolyte gel to enhance the quality of the ECG signal. The problem with this method is that the gel dries during the extended measurements, causing loss of signal quality, or patient skin irritation [1].

Until now, biopolymers that are compatible with the body have been used in research for wearable electrode design. Fabrication of biopolymers and their nanocomposite variants have been frequently investigated to avoid environmental and health effects of petrochemical equivalents and to improve the material properties.

In the study of Amberg et al., [2] a method of long-term ECG measurement was investigated. In this work, a novel textile system was used, which consisted of improved 100 nm silver-coated yarn. In the long-term, the diagnosis system involved Ag NP release to the surface of the applied tissue, and it was recognized that high Ag concentrations are cytotoxic for human cells. To be able to prevent cytotoxicity, researchers covered the surface of the electrode with a titanium adlayer. Titanium prevented cytotoxicity and provided good electrical conductivity [2].

In the study of Huang et al., a film was fabricated with Ag NWs and polydimethylsiloxane (PDMS) with a pre-staining and post-embedding process [3]. It was mentioned that the resistance to strain ratio is too high and considered as a problem that needs to be solved. This played a crucial role in the selection of Ag NW as a conductive material [3].

In the study of Weder et al., a textile electrode was demonstrated using a different method to achieve a high quality and noiseless ECG signal when the patient is in motion [4]. A polyethylene terephthalate (PET) yarn was used and plasma-coated with Ag for electrical conductivity and a titanium (Ti) layer added on top of it for the passivation of Ag. Ti was chosen because of its known passivation effect on Ag [4]. The system was moisturized with water vapor provided from an integrated reservoir that provides the system with improved electrochemical capabilities [4].

Chitosan is an important biopolymer that can be used in this application, thanks to its promising properties such as biodegradability and biocompatibility, both of which offer significant potential in medical applications. However, biopolymers are electrically insulating like most polymers, which is an obstacle for their use in ECG electrodes. Therefore, it is necessary to make them electrically conductive. So far,

nanoparticles, nanowires, nanotubes and graphene were utilized mostly as fillers to fabricate polymer-based conductive nanocomposites.

In addition to conductivity, antibacterial activity is important in medical applications. Silver historically has been known as a robust antibacterial material and has been used in many products that are required to be antibacterial [5]. With the development of nanotechnologies, different nanomaterials were tried to be realized for this purpose. For example, it was aimed to obtain Ag on a nanoscale so that it offers high surface to volume ratio. Because various methods can efficiently synthesize the zero-dimensional (0D) nanoparticles of silver, it has been produced extensively and used [6]. For example, Chen and Chiang demonstrated the large potential of Ag NPs for antibacterial textiles [7]. However, nanoparticles have some geometric limitations. For instance, their adhesion capacities are inferior due to small contact areas with the fibers of the textile. Therefore, the one-dimensional (1D) nanowires were synthesized to overcome this geometric limitation. Antibacterial properties of Ag NWs have not been extensively studied yet and there are only limited number of studies in the literature. For the first time, Liu et al. investigated the antibacterial properties of Ag NWs in aqueous solution against *Escherichia coli*, *Staphylococcus aureus* and *Bacillus subtilisin* [8]. In this work, PET substrates were covered with Ag NWs and the antibacterial performance against *Escherichia coli* was monitored [9]. Recently, Guest et al. investigated electrically conductive and antibacterial cotton textiles fabricated through Ag NW decorated [10]. More recently, Jiang and Teng have covered different amounts of Ag NWs with polydimethylsiloxane (PDMS) and showed that even a Ag NW loading of 0.2 mg could effectively destroy *Escherichia coli* and *Staphylococcus aureus* bacteria. Moreover, Ag NWs/ PDMS films showed long-term antibacterial stability [11]. Although Ag NW's antibacterial activity were evaluated in different polymer matrices, only a few studies were conducted on Ag NW/ chitosan nanocomposites and therefore this gap in literature is addressed in this thesis.

Production of functional and biocompatible Ag NW/ chitosan nanocomposite films for medical applications simultaneously require electrical conductivity and antibacterial properties. In this thesis, Ag NWs were used to fabricate antibacterial chitosan matrix nanocomposite structures. Firstly, Ag NWs were synthesized via polyol method. Morphology of the Ag NWs were examined via scanning electron microscopy (SEM). Different amounts of Ag NWs were used for the fabrication of antibacterial chitosan-based nanocomposite films. The effect of Ag NW loading on the antimicrobial performance, electrical resistance, and thermal properties of chitosan-based nanocomposites were investigated. The antibacterial performance of the nanocomposite films against *Staphylococcus aureus* (*S. Aureus,* gram-positive), *Escherichia coli* (*E. Coli*, gram-negative), *P. aeruginosa,* and *B. Cereus* were examined.

To date only a few studies have been conducted using chitosan and Ag NW nanocomposite structure, and therefore detailed materials characterization and further utilization of this nanocomposite in medical applications such as ECG electrodes have not been studied yet. This study has three main contributions to the topic. First, production of Ag NW/ chitosan nanocomposites of were demonstrated. Second, detailed materials characterization was conducted with the investigation of the antibacterial performance of the produced nanocomposites. Third, a unique demonstration of the produced nanocomposites as ECG electrodes have been made. In this comprehensive study, the results showed that, Ag NWs are promising fillers for biopolymer nanocomposites since they improve both the antibacterial activity and electrical conductivity.

CHAPTER 2

LITERATURE REVIEW

2.1. ELECTROCARDIOGRAM (ECG)

ECG has arisen as a simple and cost-effective method for monitoring the heart's electrical activity, and it only necessitates placement of a series of electrodes onto the skin or near the heart [57, 58]. Since most cardiovascular problems involve irregular heart rhythm, the ECG is a reliable tool for heart examination, it allows one to clearly distinguish between harmonic and non-harmonic electrical measurements. Additionally, ECG is a practical way to electrically activate the diseased heart to heal it [58].

The wave shapes, generated by biopotentials, which are the result of heart contractions, are called electrocardiogram (ECG) [23] as shown in Figure 2.1. The P wave is a tiny wave of deflection indicating depolarization of the atria. The PR interval is the period from the first P-wave deflection and the first QRS-complex deflection. Large Q waves refer to the interventricular septal depolarization. Q waves can also refer to respiration and are usually small and thin. They can also signify an old myocardial infarction (they are big and wide in this case). The R wave represents the depolarization of the ventricle's main mass, making it the largest wave. The S wave signals the last ventricle depolarization at the base of the ST section of the heart.

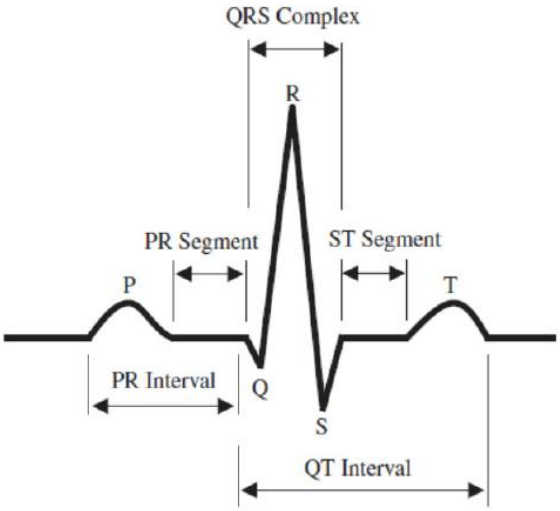

Figure 2.1 A typical ECG signal [23].

2.1.1. Electrodes

Bioelectrodes are sensors for converting ionic conductivity into electronic conductivity and making it operable within an electronic circuit. The general purpose of using bioelectrodes is to collect medically important bioelectrical markers such as electrocardiography (ECG), electroencephalograph (EEG), and electromyogram (EMG). Bioelectrodes are classified under three main groups: which are 1) surface electrodes, 2) internal electrodes and 3) microelectrodes [12].

Surface electrodes are electrodes in contact with the skin of the patient with several examples shown in Figure 2.2. The diameter of the surface electrodes ranges from 0.3 to 5 cm.

Normal skin resistances seen by the electrode vary from 0.5 kΩ for sweaty surfaces to 20 kΩ for dry skin. It can increase to 500 kΩ, especially in the case of patients with very dry or infected skin. In any case, it is necessary to think of the surface electrodes as a high-impedance voltage source, which is an important factor affecting the design of the amplifiers used to monitor biomarkers. As a general rule, the input impedance of a voltage amplifier should be at least 10 times the source impedance. In this case, the input impedance of the biopotential amplifiers should have a value of 5 MΩ or

above. This can be achieved easily using special, bipolar field effect transistors (BiFETs) or bipolar metal oxide semiconductor (BiMOS) operational amplifiers [12].

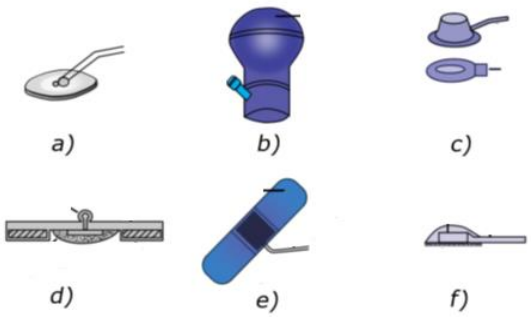

Figure 2.2 Typical surface electrodes: (a) metal plate, (b) vacuum pumped, (c) mobile type, (d) disposable, (e) bendable and (f) dry electrodes [24].

2.1.2. Electrode Connections

The standard ECG record contains 5 electrodes connected to the patient at the following locations:

- right arm (RA),
- left arm (LA),
- left leg (LL),
- right leg (RL),
- chest (C).

These electrodes are applied to a buffer amplifier with a differential input via a connection select switch [50-55,62]. The ECG takes the patient's right leg as the reference electrode. The desired connection type (I, II, III, AVR, AVF and AVL) is selected by the connection selector switch. Bipolar connections are called I, II and III and form the Einthoven triangle as shown in Figure 2.3 and with details as follows:

1. aVR lead connected to the RA
2. aVL lead connected to the LA

3. aVF lead connected to the LL

4. Connection 1: When connecting the LA electrode to the non-inverting input of the amplifier, RA is connected to the inverter input.

5. Connection II: LL is connected to the non-inverting input of the electrode while RA electrode is connected to the non-inverting input of the amplifier (LA is connected to RL).

6. Connection III: LL is connected to the non-inverting inlet; LA is connected to the inverted inlet (RA is connected to the RL).

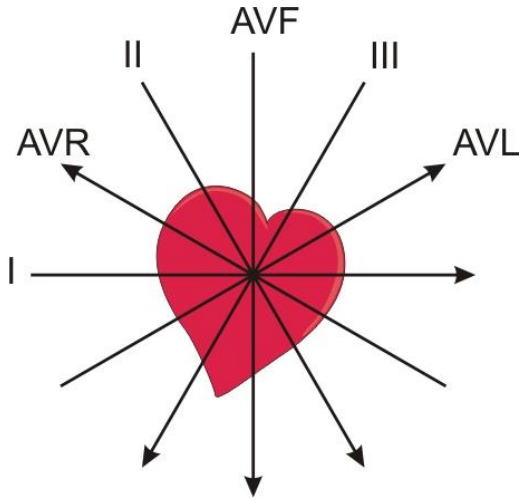

Figure 2.3 Cardiac axis observed by standard connections [12].

In unipolar chest connections (voltages from V1 to V6), the voltages from various points of the chest are given to the non-inverting input of the amplifier, while the signals from the RA, LA and LL points are collected with a Wilson circuit and measured by connecting the amplifier to the inverter input [12].

2.2. Polymers used in Electrode Production

Polymers are basically chains that are consists of repeatedly gathered monomers units and they have strong intermolecular interactions [12]. The intermolecular interaction type, which varies significantly from polymer to polymer, plays a prominent role in determining the properties of the polymers. Depending on whether the polymer chains are nicely ordered or disorganized, polymers are also classified as either crystalline, semi-crystalline or amorphous [13].

2.2.1. Characteristics of Crystalline, Semi-Crystalline and Amorphous Polymers

Amorphous polymers typically exhibit a crystallinity less than 10% and crystalline polymers typically contain more than 80% crystalline structures. Semi-crystalline polymers display a crystallinity ranging from 10 to 80% [14]. They are also classified through their glass transition temperature (Tg) and melting temperature (Tm) into those different groups. The amorphous polymers do not have a clear melting point in this respect and their glass transition temperatures are between −125 and 350 ° C. On the other hand, semi-crystalline polymers have a distinct Tm, while their Tg, in general, is higher than amorphous polymers and typically in the range of 75 to 260 °C [15]. On the other hand, highly crystalline polymers exhibit a Tm and do not have any Tg associated to them. Crystalline polymers have high stability, strength, and good environmental stability [16,17]. Crystalline polymers have well-ordered molecular arrangements which limits their molecular chains mobility. Therefore, crystalline polymers are mechanically stronger and rigid. But this makes them not suited for flexible electronics [18,19].

2.2.2. Structure of Chitosan

Chitosan is a linear polysaccharide consisting of (1-4) linked D-glucosamine units, which is the result of deacetylation of the chitin in the alkaline medium. Figure 2.4

shows the molecular structure of chitin and chitosan. Chitin, [ß- (1-4) -poly-N-acetyl-D-glucosamine], is the base material of skeletons of arthropods and is also found in the cell wall of some bacteria and fungi. Instead of the hydroxyl group in the C2 carbon, there is a group of acetamido in the cellulose.

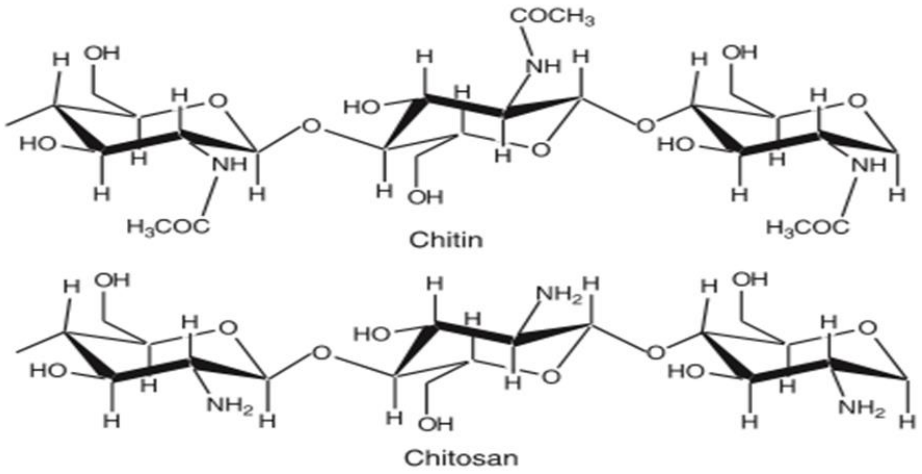

Figure 2.4 Molecular structure of chitin and chitosan [19].

In recent research of Liu et al., a wearable sensor based on chitosan fabric, was fabricated by electroless deposition of silver nanoparticles onto the fiber.[29]. Quite low electrical resistance of 1 Ω/sq was observed due to the strong reaction between the amine groups of chitosan and Ag ions.

The main motivation of this research is to come up with an alternative electrode that allows long-term ECG observation. A new type of electrode is investigated since Ag/AgCl electrodes are not suitable for long-term ECG measurements. Driving force here is to measure ECG signals during daily life and at night in hopes to provide data for sudden cardiac arrests happening at marathons or at night because of sleep apnea.

Two main challenges were confronted during the fabrication process. The first problem was the delamination of the metal layer from polymer/fiber surface.

Because of abrasion and wash, delamination causes high conductivity loss. The second problem was related to the application of the conductive polymers/fibers, because it is almost impossible to fabricate flexible and conductive polymers/fibers [33].

Chitosan is a promising candidate for wearable electrodes since its amine group is highly active towards metal ions, which allows some conductivity and antibacterial properties. In previous research, Ag NPs were electrolessly plated onto the surface of chitosan fabrics [33].

The morphology of Ag-plated chitosan fibers can be seen in the SEM images provided in Figure 2.5.

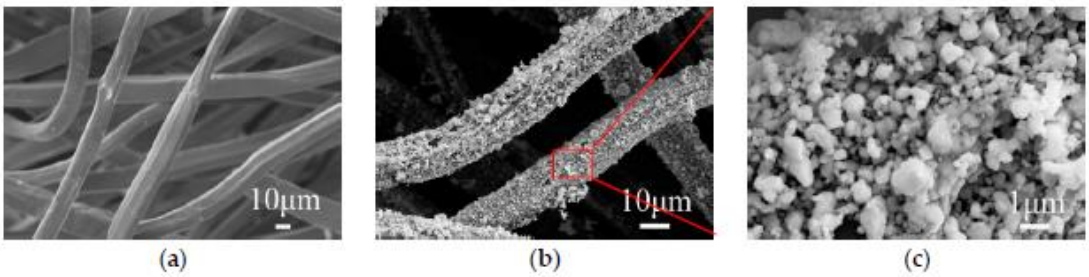

Figure 2.5 SEM images of (a) pristine and (b, c) Ag-plated chitosan fibers [33].

Electrical resistance is a very important factor for ECG measurements. Tests on silver nitrate ($AgNO_3$) were conducted to observe the electrical conductivity related to the Ag NP deposition on chitosan fabrics. The effect of Ag concentration on the conductivity can be seen in Table 2.1. Electrical resistance is found to decrease as $AgNO_3$ concentration increases. Also, electrical resistance of conductive chitosan fabric is much lower compared to cotton and silk fabrics [33].

Table 2.1 Effects of $AgNO_3$ concentration on Ag content and electrical resistance (Adapted from [33]).

AgNO3	5% wt.	7.5% wt.	10% wt.	12.5% wt.	15% wt.
Weight of Ag-plated fabrics (g)	0.31 ± 0.01	0.38 ± 0.03	0.44 ± 0.06	0.52 ± 0.03	0.61 ± 0.05
Silver Content (g/g)	0.30 ± 0.01	1.01 ± 0.02	1.22 ± 0.05	1.48 ± 0.05	2.08 ± 0.08
Electrical resistance (Ω/sq)	0.1499 ± 0.0485	0.0700 ± 0.0103	0.0565 ± 0.0115	0.0443 ± 0.0051	0.0332 ± 0.0041

The system used for testing can be seen in Figure 2.6. Conductive fibers were hot pressed onto the ECG-shirt and measurements were taken during static, jogging and running states.

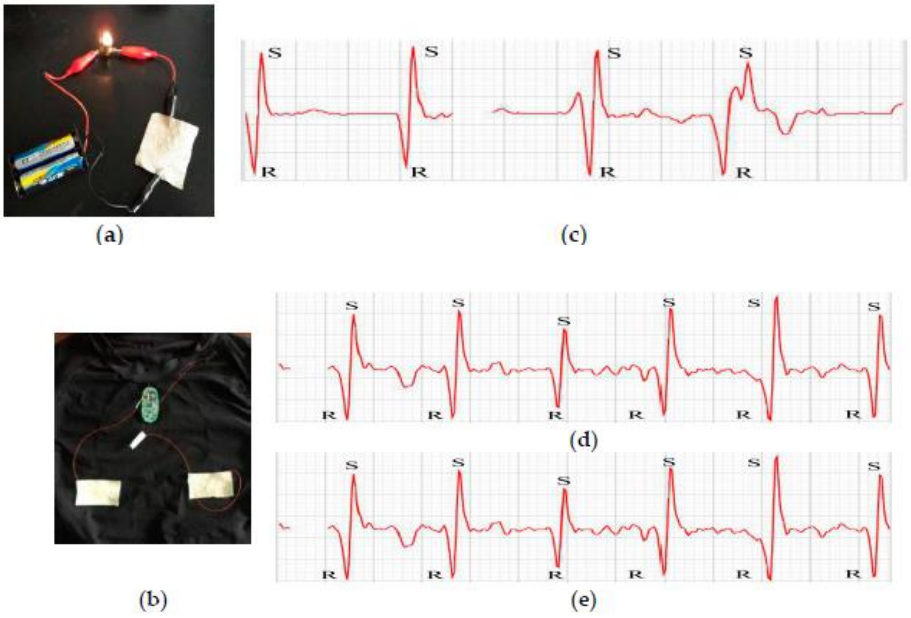

Figure 2.6 Application of conductive chitosan fabrics in smart garment (a) photograph of garment, (b) the inside of the garment, (c) static state (0 km/h), (d) jogging state (3 km/h) and (e) running state (12 km/h) [33].

Chitosan fabric was washed for eight times for testing purposes and its conductivity remained below 1 Ω/sq [33]. It has been concluded that the chitosan fabrics have capabilities for long-term ECG measurement as a smart garment.

2.3. Nanofillers and Materials Used in Wearable Electrode Applications

In Table 2.2, ECG and EMG electrode applications, integration of conductive materials and systems to the body for daily use as well as electrode locations are summarized. Various conducting materials were used such as Ag, gold, stainless steel and Ag coated and Ag-plated yarns. Also, various electrode locations were investigated. The way to bridge the existing difference between conductive polymers and their inorganic equivalents is by using inorganic fillers to reinforce them. 2D and 1D nanomaterials are the main components of most of today's inorganically reinforced polymers [20]. There is a wide range of such materials. The most studied are 2D graphene sheets and 1D carbon nanotubes (CNT) and silicon nanowires.

Table 2.2 ECG electrode studies from literature (Adapted from [57]).

Biopotential Signal	Manufacturing Technique	Conductive Material	System Integration	Electrode Location
ECG	Electroless plating	Silver Nanoparticles	Smart garment	Lead 1 and2
ECG	Sputtering, electroless plating, knitting, and embroidering	Cu, Ni, stainless steel,filament, nylon,fabric	T-shirt	Chest
ECG	Graphene-coated textile	Graphene	Wristband	Left and Right arms
ECG	Printing	PEDOT:PSS	Kimono	Chest and Wrists
ECG	Weaving and knitting	Silver Yarns,	Chest Band	Chest
ECG	Knitting	Silver,Stainless Steel Yarn, Copper Filaments	Garment Band	Lead 1
ECG	Knitting, embroidering, and weaving	Silver	Elastic Belt	Chest
ECG	Knitting	Stainless Steel	Belt	Chest
ECG	PVD	Ag/Ti PET Yarn	Belt	Chest
ECG	Conductive thread	Silver:PEDOT PSS	Bras	Lead 1-to3
ECG	Printing	Silver	Chest Band	Chest
ECG	Ink-jet printing	Graphene	T-Shirt	Finger
ECG	Commercial textile	Silver	T-Shirt	Lead 1-to3
ECG	Screen printing	Silver Paste	Band-Aid	Chest
ECG	Knitting	Silver Coated Yarns	Swim Suit	Chest
ECG	Commercial textile	Silver and Gold	Smart Jacket	Chest
ECG	Knitting and woven	Stainless Steel	Baby Suit	Back
ECG	Knitting	Stainless Steel Threads	T-shirt	RA,LA,LL,RL,V1-V6
EEG	Seamless knitting	Ag-AgCl Coated Thread	Head Band	Forehead
EEG	Screen printing	Carbon-Loaded Rubber	Head Band	Forehead
EEG	Screen printing	Ag-particle,fluoropolymer composite ink,	Stand Alone	Behind Ears
EMG	Knitting	Silver Plated Yarn	Band	Flexor Carpi Ulnaris
EMG	Knitting	Silver Plated Naylon	Shirt	Biceps and Triceps

2.3.1. Graphene

Graphene consists of carbon atoms which forms monolayer. Typically, they have 2D hexagonal honeycomb lattice structure by packed with a bond length of around 1.42 Å [21] and their thickness is around just one atomic layer (approximately 0.3 nm), that makes them the "thinnest" materials ever [22]. Those 2D nanomaterials show highly strong electrical conductivity [23], also they have perfect thermal conductivity (up to 3000 W m^{-1} K^{-1}) [54]. Furthermore, they have reliable mechanical stability (ultimate tensile strength (130 GPa) and high Young's modulus (1 TPa) [23,24] Morevoer, they have small thermal expansion coefficient (CTE) (10^{-6} K^{-1}) [25,26].

2.3.2. Carbon Nanotubes (CNTs)

CNTs are formed up of graphene sheets that are rolled up into high-aspect-ratio (more then 1000) tubes [29]. They come as single-wall carbon nanotubes (SWCNTs) and multi-wall carbon nanotubes (MWCNTs) and show peculiar properties. For instance, tensile strength of SWCNTs is significantly lower than that of MWCNTs. MWCNTs are always metallic, while SWCNTs can be both metallic and semiconducting depending on the orientation of the graphene sheet.

The excellent properties of CNTs have made them into commonly used nanofillers in polymer matrixes for the production of elastic, stretchable and deformable electronics [30, 33–34]. Many approaches have been developed to integrate CNTs into polymers, such as liquid mixing, melt processing and in-situ polymerization [31]. Untreated CNTs; however, are chemically inert.

In another research by Liu et al., instead of metal electrodes, a polymer matrix composite electrode was evaluated for ECG measurements consisting of PDMS

loaded with CNTs and Ag NPs. Samples were prepared via ultrasonic and heat-stirring technique as shown schematically in Figure 2.7 [31].

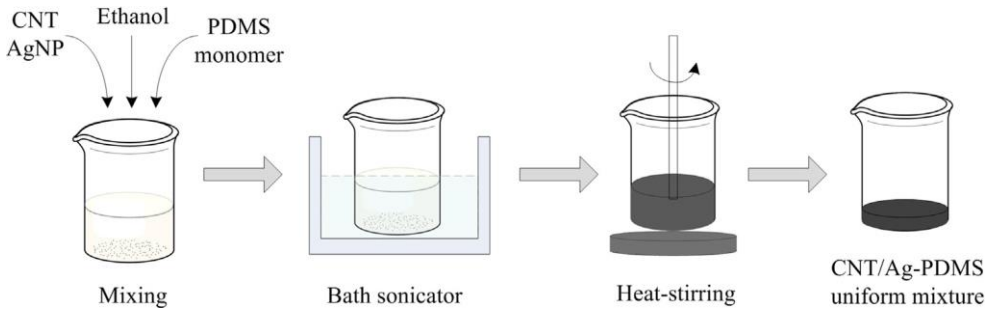

Figure 2.7 The fabrication process of the conductive polymer mixture [10].

For measurements, conductive wires were sewn onto CNT/Ag-PDMS to obtain wearable electrodes [31]. This previous study also mentions the existence of Au layered foam electrodes and argues that fabrication of such electrodes to be expensive.

PDMS was selected as the base and CNTs were embraced as fillers. CNTs were randomly incorporated, providing a good network within the polymer matrix. Lastly, embedding of nanoparticles, in this case Ag NPs, increased the stretchability of the sample. Wearable electrodes were fabricated from this sample and tested. Photos of these electrodes can be seen in Figure 2.8 [31].

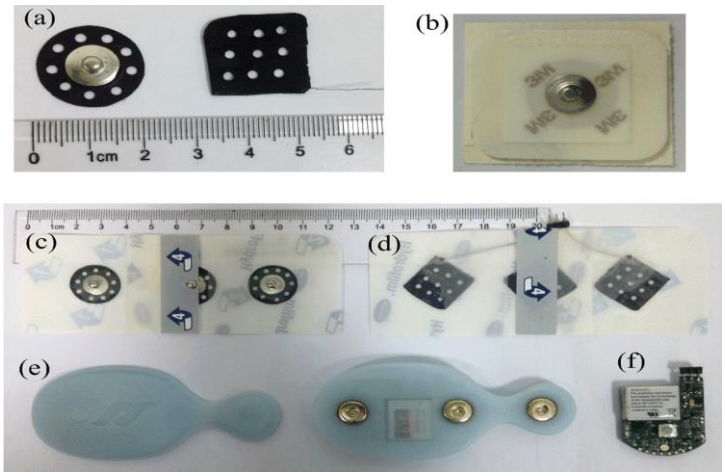

Figure 2.8 Photographs of (a) CNT/Ag-PDMS electrodes with different shape, (b) Ag/AgCl electrode; three-electrode patch with (c) round electrodes and (d) square electrodes, (e) front- and back-side pictures of the measurement system encapsulated into a silicone shell. (f) The circuit system used in this study and coupled with patch (d) [10].

For ECG measurements, researchers used a 3 electrode-patch, sewn into a vest. Figure 2-9 shows the measurement results obtained using different composite electrodes.

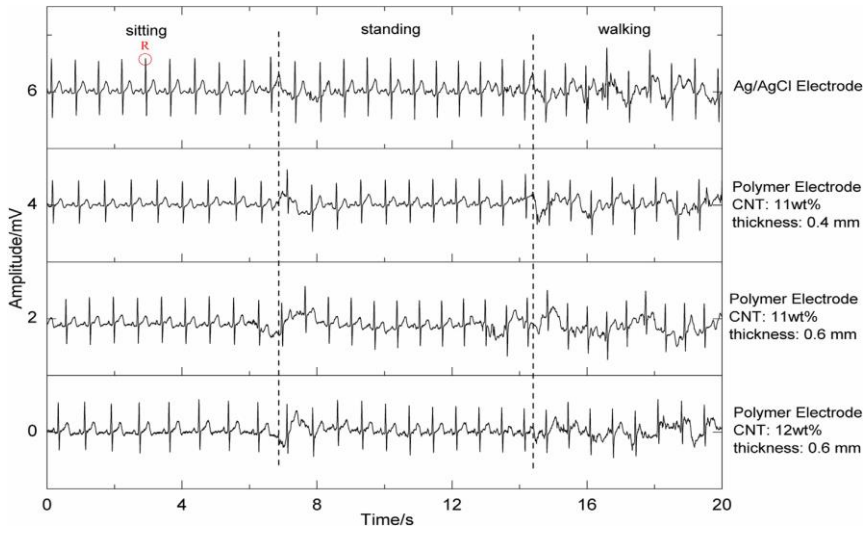

Figure 2.9 ECG measurement results. The dashed lines show the signal changing when the subject changed his body posture [10].

Following measurements, it was realized that the amplitude of the signals acquired with Ag/AgCl electrodes were higher. This was due to the lack of electrolyte for

polymer electrodes [31]. The effect of electrode thickness was also investigated. Thicker electrodes managed to achieve a higher amplitude signal. In addition, electrodes with higher CNT content provided signals with higher amplitude as well. As usual with general ECG measurements, tests were conducted in different positions to examine how well the electrodes perform when there were high motion artefacts as represented in Figure 2.10.

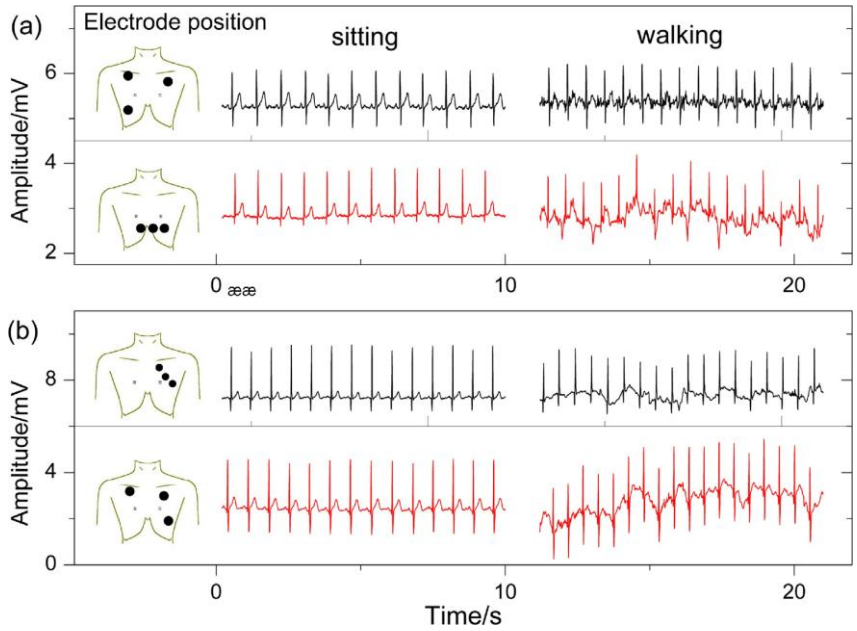

Figure 2.10 ECG measurement results of wearable electrodes with different positions for a (a) female and (b) male subject [10].

Long-term measurements were also acquired. Electrodes were worn daily for 14 days; countable ECG results were acquired and skin capability was tested as shown in Figure 2.11 [31].

Signal amplitude was found to decrease as the days passed due to the adhesive. As days pass, adhesive of the electrode got weaker, which led to a loss in signal amplitude and increased motion artefacts [31]. Overall, polymer electrodes showed a promising future in long-term ECG measurements.

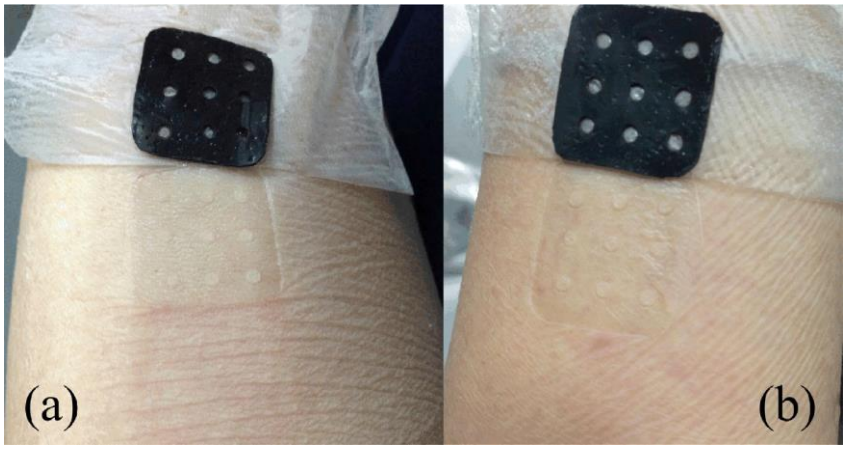

Figure 2.11 Photographs from skin compatibility test. The square electrodes were attached on the forearm. After (a) 1 week and (b) 2 weeks, no skin irritation was observed at either electrode contact area [10].

2.3.3. Silver Nanowires (Ag NWs)

Ag NWs are another fascinating group of metallic nanomaterials, commonly used in different types of wearable and versatile bioelectronics [36,32–34]. Ag NWs can form highly conductive percolative networks in both 2D and 3D structures to provide good optical visibility and high structural versatility simultaneously.

Ag NWs are very popular in bio-signal sensing because of their antibacterial properties. In the study of Myers et al, Ag NWs have been used as a dry electrode. Dry electrodes are available, but they have several setbacks. They are uncomfortable to wear and the absence of electrolyte gel between the electrode and skin results in high impedance between in between. One of the main problems this study attempts to solve is the motion artefacts. Microneedles suffer from this problem the most and thus prevents their long-term use. Non-invasive methods also have motion artefacts because of metal delamination from the surface or lacking conformal contact with the skin. Even though it is a dry electrode, it is said to be stretchable and thus provides a solution towards skin contact [27]. Electrode fabrication was done by pouring PDMS on a network of Ag NWs and then a compatible ECG equipment was pressed onto the mixture, as schematically shown in Figure 2.12 [27].

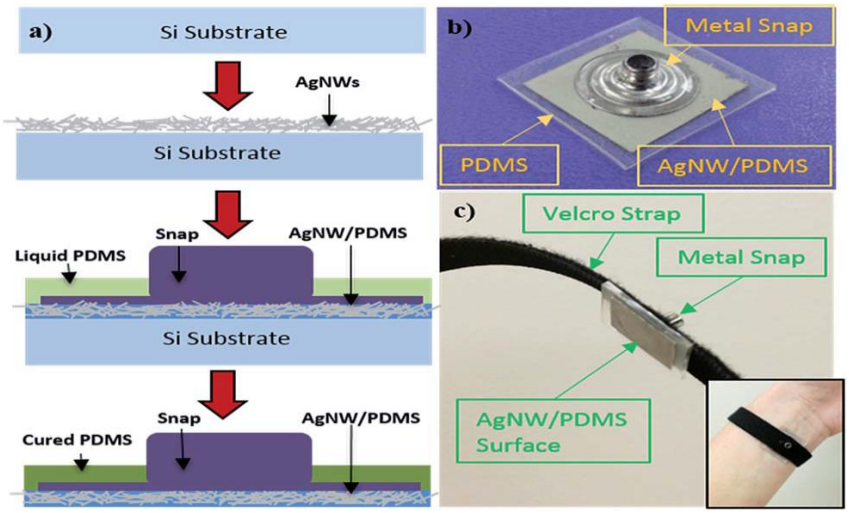

Figure 2.12 (a) Schematics of the fabrication process of the Ag NW dry electrodes. (b) Ag NW dry electrode with a metal snap. (c) Ag NW dry electrode with Velcro strap for ECG measurements [7].

Prior to the signal quality tests, impedance was measured as a function of pressure. As shown in the Figure 2.13, impedance was found to decrease with pressure [27].

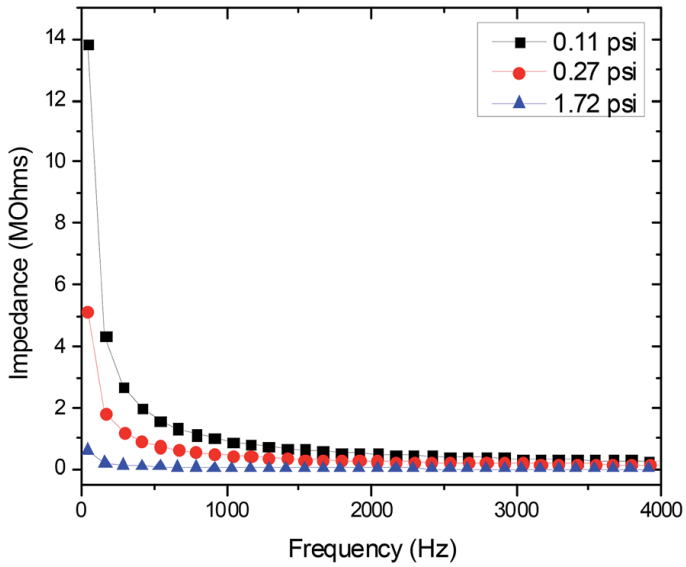

Figure 2.13 Electrode-skin impedance with increasing application pressure [27].

Multiple tests were conducted with the subject being in several different positions. Tests results were acquired for both ECG and EMG. For ECG, first set of data were

acquired from tests with no movement, then tests were conducted with one-degree of movement and lastly tests were conducted with two-degrees of movement. EMG tests were performed with a wrist-extension test. ECG signals were plotted only using the default settings of the amplifier with no additional signal processing involved. Noise and quality comparison of dry and wet electrodes can be seen in the Figure 2.14. Even though the dry electrode had more noise, it provided a better signal quality. The reason behind this was the sliding of the wet electrode due to the electrolyte gel [27].

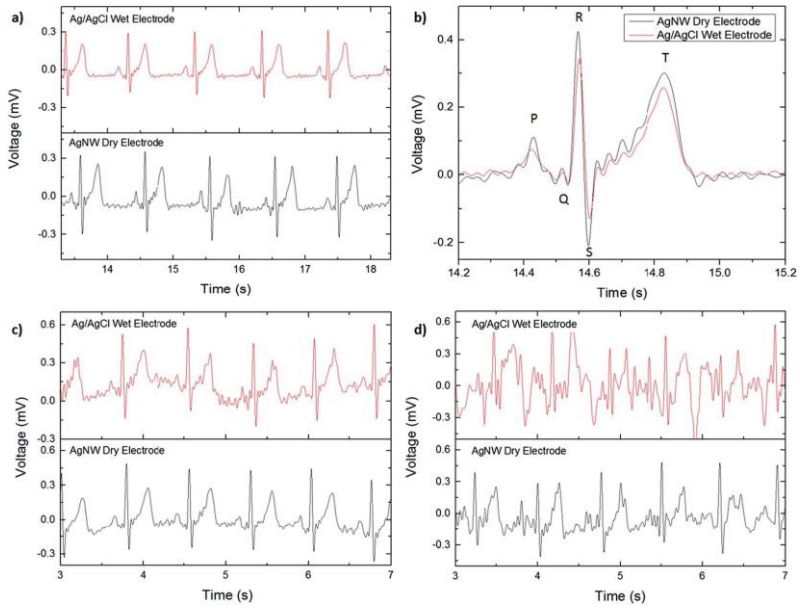

Figure 2.14 (a) ECG recording of Ag/AgCl wet electrode and Ag NW dry electrode taken while subject was seated and resting. (b) ECG signal comparison of the P, Q, R, S, and T waves between the Ag/AgCl electrode and NW electrode. (c) ECG signal comparison of the subject swinging their arms, one degree of movement. (d) ECG signal comparison of the subject jogging, two degrees of movement [7].

Electrodes using Ag NWs embedded into PDMS substrates were also used for long-term ECG measurements with no noticeable degradation of the electrodes or irritation of the skin. Since the Ag NWs were embedded in the PDMS substrate, they were also more resistant to oxidation. In summary, Ag NW dry electrodes showed excellent performance in both ECG and EMG measurements. Quality signals were produced on par with wet electrodes and there was no skin irritation or discomfort while wearing the electrodes [27].

CHAPTER 3

EXPERIMENTAL DETAILS

3.1. Materials

Chitosan with the medium molecular weight was purchased from Sigma Aldrich and used without further purification in this thesis. Molecular weight and degree of deacetylation are presented in Table 3.1 according to the technical datasheet. Poly (vinylpyrrolidone) PVP (MW = 55000), ethylene glycol (EG), silver nitride ($AgNO_3$), sodium chloride (NaCl, % 99.5) used for Ag NW synthesis were also purchased from Sigma Aldrich. These materials were used without further purification.

Table 3.1 Material properties of chitosan.

Chitosan type	Molecular Weight	The degree of deacetylation	Solvent used
Chitosan (Medium, Sigma Aldrich)	190-310 kDa	% 75-85	% 1 lactic acid
Chitosan (DAC 100, Koyo Chemical)	235 kDa	100%	% 1 lactic acid

3.2. Ag NW Synthesis

Ag NWs were synthesized using the polyol method, similar to the work of Coskun et al [74]. First, 0.12 M $AgNO_3$ was prepared and mixed in 40 ml of EG solution with a magnetic stirrer at ambient temperature. Following the preparation of $AgNO_3$ /EG solution, the solution was placed in an oil bath at 120 °C. In the meantime, 80 ml of EG solution was prepared with 0.45 M PVP and 1 M NaCl. This solution was stirred at 120 °C until all the constituents were dissolved and cooled to room temperature.

Afterwards, PVP/EG solution was added onto the $AgNO_3$ solution, and the bath temperature was increased to 160 °C. Solution was held there for 90 minutes. Following synthesis, Ag NWs were purified by centrifuging at 7500 rpm twice and they were redispersed in distilled water for further utilization as shown in Figure 3.1.

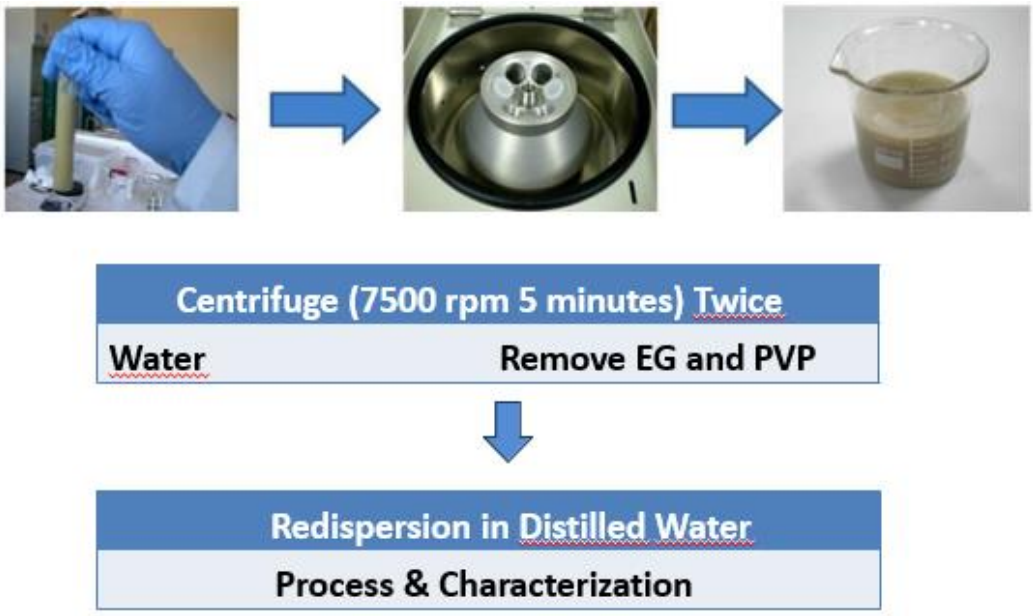

Figure 3.1 Schematics of Ag NW purification steps [modified from 54].

3.3. Nanocomposite Preparation

Chitosan/Ag NW composite films were produced by a simple solvent casting method. Lactic acid with a concentration of 1 vol. % was used as a solvent for the fabrication, stirred until it takes a gel form, and then evaporated using a vacuum oven as illustrated in Figure 3.2. While chitosan has low solubility in aqueous solutions and organic solvents, it is soluble in a strong organic acid. The most widely used acids include formic acid, acetic acid and lactic acid [36,37,38,39]. In this study, lactic acid was used as a solvent to form a gel. Also, glycerol was used as a plasticizer to make stretchable elastic films and composite electrodes.

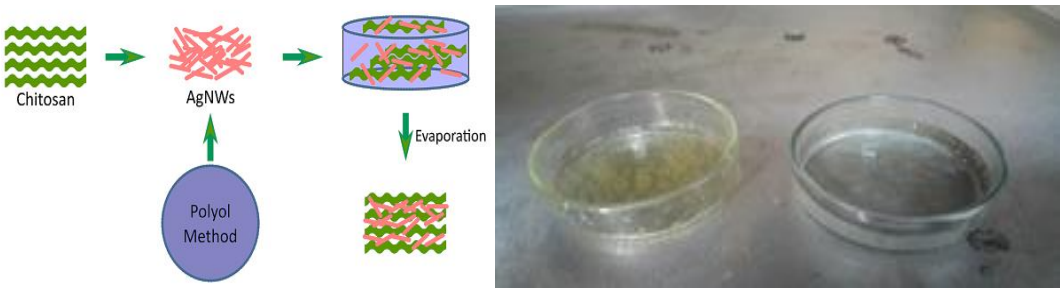

Figure 3.2 Chitosan/ Ag NW nanocomposite film production steps (left) and photos of produced films (right).

Seven different samples were prepared for the characterization. The production parameters are provided in Table 3.2.

Table 3.2 *Materials and their amounts used to produce nanocomposite films and electrodes.*

Parameter	Chitosan	Lactic Acid (1 vol. %)	Glycerol	Ag NW
Unit	mg	ml	ml	mg
Neat	250.00	12.50	0.50	0.00
1wt.%	250.00	12.50	0.50	2.52
2wt.%	250.00	12.50	0.50	5.10
4wt.%	250.00	12.50	0.50	10.41
10 wt.%	250.00	12.50	0.50	27.28
20 wt.%	250.00	12.50	0.50	62.50
40 wt.%	250.00	12.50	0.50	166.67

Each sample was poured onto a glass petri dish with a diameter of 60 mm, half filled with containers (0.7 mm height) and kept at 50 ^{0} C and 0.06 MPa pressure for 40 hours.

Composite Electrodes Preparation

Figure 3.3 shows the ECG electrode production steps, which are similar to those for composite film production. Before placing the electrodes into the vacuum oven, metal snaps that are compatible with ECG devices were embedded into the jellies while in the petri dish. Each concentration contained eight metal snaps, which means eight electrodes were produced at each concentration. Four electrodes were randomly chosen for each ECG test and their performances were evaluated as described in Section 4.

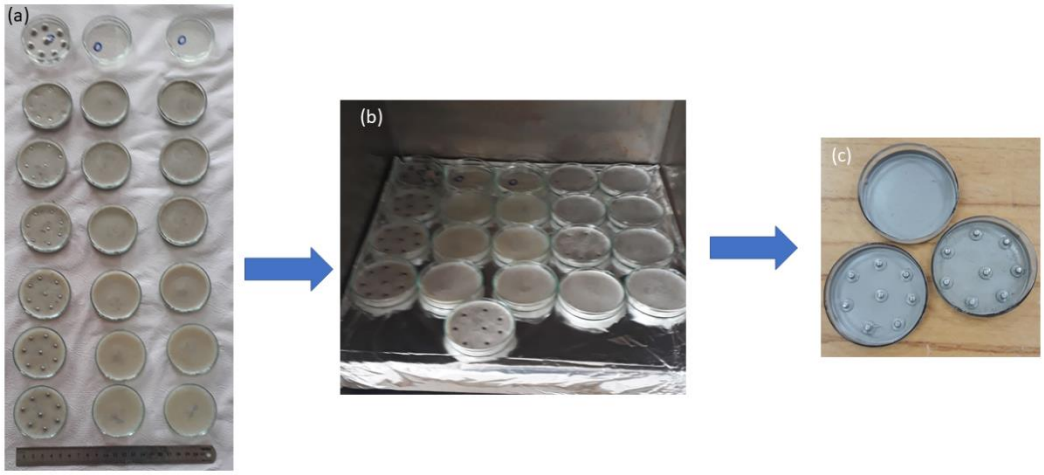

Figure 3.3 Photographs of chitosan/ Ag NW nanocomposite electrode production steps; (a.) solvent casting, (b) evaporation in an oven, (c) shaping to use in ECG equipment.

Figure 3.4 shows the photographs of standard, commercially available AgCl wet electrodes, which were used in this work as control samples to compare the performance of Ag NW/ chitosan nanocomposite electrodes. The brand of these electrodes was “Beybi”. These electrodes had a diameter of 55 mm and came with a jelly electrolyte. A 10 mm diameter sensitive area was used in the experiments conducted in this thesis.

Figure 3.4 A photograph of standard, commercially available Ag-Cl wet electrodes.

3.4. Characterization of Nanocomposites

3.4.1. Differential Scanning Calorimetry (DSC)

To determine the crystallinity and transition temperatures of the Ag NW/ chitosan composites, DSC analysis was performed. It is important to determine the crystallinity and transition temperatures of the electrodes, which in turn provides insights on optimum operational temperatures. For this purpose, Trios-SDT 650 simultaneous DSC system was used and nitrogen atmosphere was employed for the analyses.

3.4.2. Thermogravimetric Analysis (TGA)

TGA shows weight loss of the composites with temperature. The point with dramatic weight loss determines the degradation temperature of the composites. In this thesis 10° C / min heating rate from -50 ° C to 600 ° C heating range was employed.

3.4.3. Scanning Electron Microscopy Analysis (SEM)

The morphology of the nanocomposites, Ag NW's, distribution and orientation of Ag NWs has prime importance in the reproducibility of the samples. Therefore, each sample was characterized by SEM before antibacterial tests. SEM ("FEI Nova Nano SEM 430") was used to determine the morphology and orientation of Ag NWs within the chitosan matrix. SEM was operated under an accelerating voltage of 5 kV. A thin gold layer (5 nm) was deposited onto the samples prior to SEM analysis.

3.4.4. Fourier Transform-Infrared (FTIR) Spectroscopy

The attenuated total reflectance (ATR) unit of the FTIR spectrometer (Perkin Elmer 400) with a scanning number of 16 with a resolution of 4 cm^{-1} was used within a wavenumber range of 400 - 4000 cm^{-1} to investigate the potential interfacial interactions between Ag NWs and chitosan within the fabricated composites

3.3.5. Electrical Conductivity Measurements

Nanocomposite resistivity was measured using Keithley 2400 source meter (Keithley Instruments, INC.). A Swagelok cell was used to measure nanocomposite films resistivity along their thickness. For the measurements, three different circular specimens were used with a radius of 10 mm for each concentration. Afterwards, the following formula was utilized to obtain electrical conductivity values:

$$\sigma = t / (R \times A)$$

where σ is DC conductivity, *R* is resistance, *A* is area and *t* is the thickness of the specimen, accordingly.

3.5. Antimicrobial Performance Evaluation

Staphylococcus aureus (ATCC #25923), *Escherichia coli* (ATCC#25922), *Bacillus cereus* (ATCC#14603) and *Candida albicans* (ATCC #90028) strains were used in this study. *Staphylococcus aureus* were cultured on 5% sheep blood agar (Orbak, Ankara, Turkey), *E. coli* and *B. cereus* were grown at an equal amount of 20 ml Mueller Hinton agar (Merck, Germany) and *C. Albicans* were cultured on Sabourraud dextrose agar (SDA) (Merck, Germany) at 37°C for 24–48 hours aerobically. Then, freshly grown bacterial and fungal colonies were harvested and prepared bacterial and fungal suspensions were prepared in sterilized test tubes containing brain heart infusion broth for *S. aureus*, *E. coli*, *B. cereus* and Sabourraud dextrose broth (SDB) (Merck, Germany) for *C. Albicans*. The final concentrations of the bacterial strains were adjusted to 1.5 x 10^8 CFU/ml and the final concentration of fungal suspension was adjusted to 2.5 x 10^3 CFU/ml according to the turbidity of McFarland test standards. Additionally, the inoculums were adjusted according to their Optical density (OD450nm: 0,600) spectrophotometrically, also. For *S. aureus*, *E. coli* and *B. cereus* Mueller Hinton agar (Merck, Germany) and for *C. Albicans*, SDA were prepared, and 100 µl amount of the freshly prepared inoculums were poured on the sterilized Petri plates. Each of the strains was spread on their specific agar plates. Then, 10 of each material (0, 1, 2, 3, 4, 5, 6) were placed onto the agar plates. Then, bacterial and fungal strains were incubated at 37°C for 24 - 48 hours aerobically. At the end of the incubation time, the diameter of inhibition zones was measured with a digital caliper (Mitutoyo, SP, Brazil) by a blinded, independent observer. The test results were calculated as arithmetic mean numbers, and the results were assessed employing Origin data visualization software.

3.6. ECG Measurements

ECG measurements were conducted with a commercial device PC-based ECG system. “A EKG Master USB mini-acquisition module” is the main component of the PC based ECG system. Figure 3.5 represents the USB PC based ECG system and its connections. As can be seen in the figure, the device is a portable unit. This module acquires and transports 12 lead standard ECG signals to the PC. This is performed with SW recording and tracking of the specially developed driver and Win EKG Pro. Using Windows operating system, the EKG Master USB and dedicated Win EKG Pro software work on desktop or notebook computers. With its mounted 5 m length unique cable, it is linked to the PC. Using one of the specified display formats, ECG information will be tracked on-screen. In the same manner, a printer compatible with Windows can be used to print out the data.

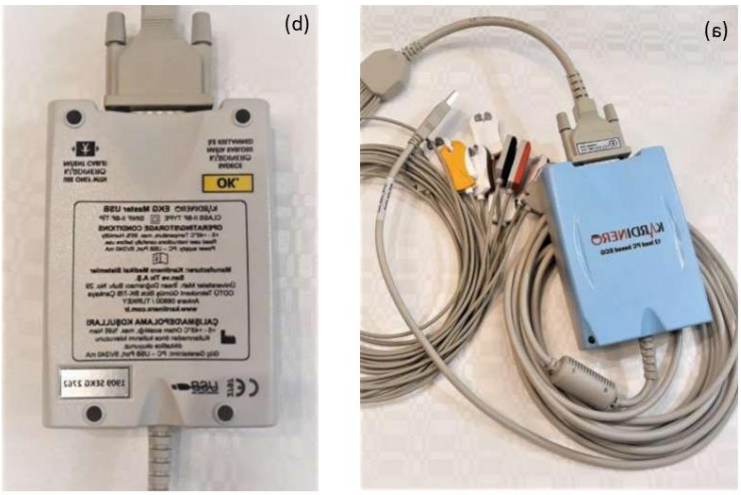

Figure 3.5 ECG Master USB PC Based ECG System.

As can be seen from Figure 3.6, there are two sides to the ECG procurement circuitry: an isolated side and a non-isolated side. A DC-DC converter power supply and signal isolation optocouplers separate these sides. The non-isolated side includes PC link

circuits. One ECG cable to be connected to the device contains resistors at the tips, to guarantee defibrillator protected inputs.

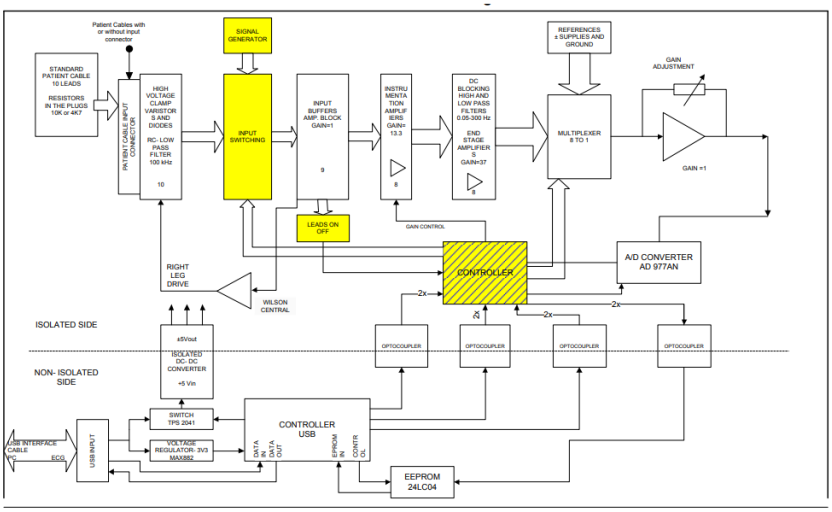

Figure 3.6 Control diagram for ECG Master USB PC Based ECG System.

The cable connector is a D-sub 15 pin connector, with a specially designed configuration. Figure 3.7 shows the locations of the electrodes tested. Four electrodes with different Ag NW amounts were used each time and the standard wet electrodes with the same location were utilized to compare the results.

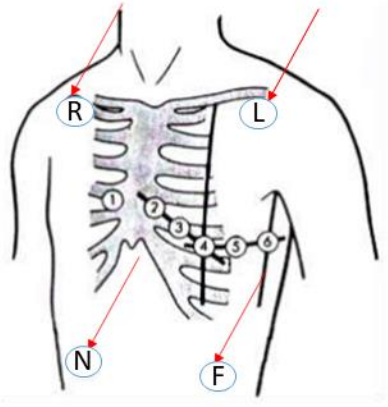

R (RA), Red, Right arm
L (LA), Yellow, Left arm
F (LL), Green, Left leg
N (RL), Black, Right leg
C1, Red, 4th intercostas space to the right of the chest bone,
C2, Yellow, 4th intercostals space to the left of the chest bone,
C3, Green, in the middle between C2 and C4, 5th costal bone,
C4, Brown, 5th intercostals space, mid line below the left clavicle,
C5, Black, same level like C4, frontal armpit line,
C6, Violet, it level like C4, mid armpit line.

.

Figure 3.7 *Locations of the electrodes tested in this study.*

CHAPTER 4

RESULTS AND DISCUSSION

4.1.1. Distribution of Ag NWs in Chitosan Matrix

SEM images of nanocomposites with different Ag NW contents are shown In figure 4.1. SEM images presented have the same magnification. As expected, with the increase in the Ag NW loading, nanowires become more evident in the images. As can be seen from the figures, Ag NW's are homogeneously dispersed within the chitosan matrix, which is important for the fabrication of reproducible and high sensitivity ECG electrodes. In terms of ECG electrode production, the significance of dispersion is explained in Section 4.5.

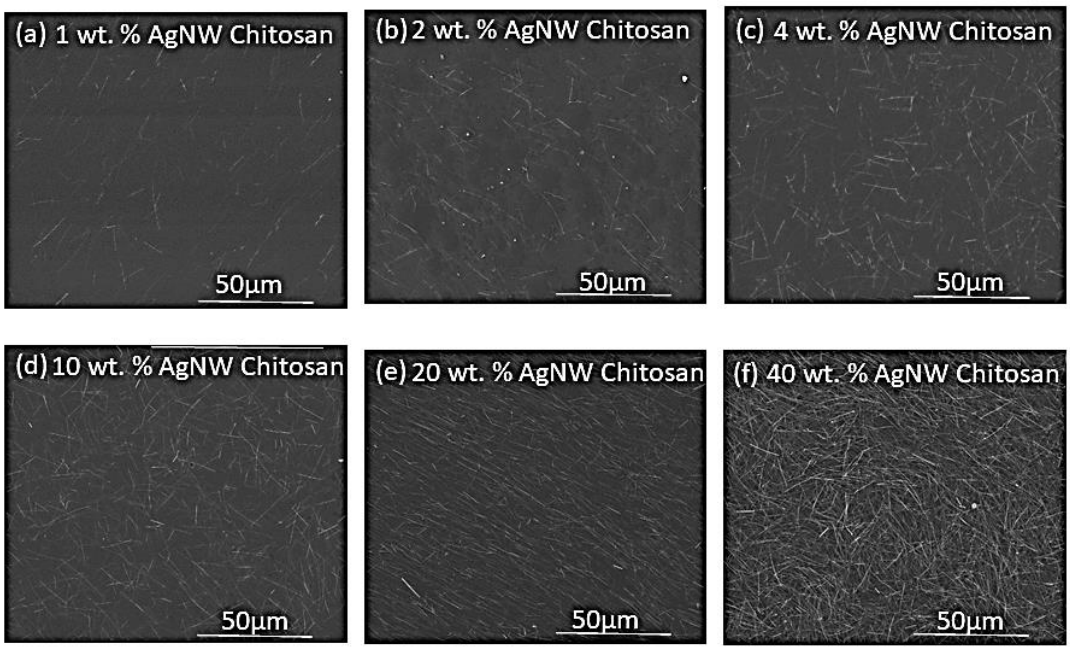

Figure 4.1 SEM images of Ag NW/ chitosan nanocomposites with Ag NW loadings of (a) 1 wt. %, (b) 2 wt. %., (c) 4 wt. %., (d) 10 wt. %, (e) 20 wt. % and (f) 40 wt. %.

4.1.2. FTIR Analysis

Figure 4.2 shows the FTIR analysis results for bare chitosan and Ag NW/ chitosan nanocomposite films. The raw data were modified with baseline correction method to get the results. Small peaks visible in the 2300 - 1800 cm^{-1} range belong to the ATR crystal and were not evaluated for the sample. A band in 3270 cm^{-1} represents combined peaks of NH_2 and OH groups stretching vibration in chitosan. For Ag NW/ chitosan nanocomposite films the peak shifted to 3261.3 cm^{-1} and peak became narrower, which signifies the reduction of hydrogen bonding.

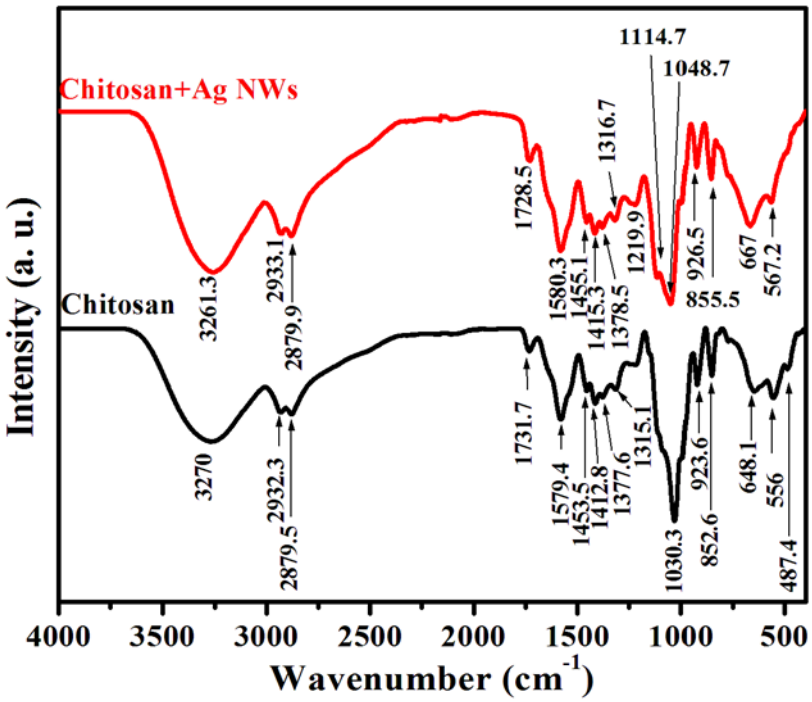

Figure 4.2 FTIR analysis results for bare chitosan and Ag NW/ chitosan nanocomposite films.

4.2. Thermal Analysis

4.2.1. Differential Scanning Calorimetry (DSC)

DSC was performed for the thermal characterization of the fabricated nanocomposites. Endothermic and exothermic peak points with their possible reasons were elaborated. The results were validated with literature. Table 4.1 shows the DSC analysis of chitosan and composite materials. In the literature, analyses were conducted with various heating rates such as 20 °C/min, 10 °C/min and 5 °C/min. Endothermic and exothermic peak points were observed around 100 °C and exothermic peak points ranged between 230 °C and 340 °C.

Table 4.1 Thermal properties through DSC analysis for chitosan and composite materials in literature.

Ref.	Chitosan used/compared	Endothermic peak*	Exothermic peak*	Heating Range	Heating Rate
[37]	Chitosan and silver loaded chitosan nanoparticles (slcn)	66°C – 130°C (Chitosan) 100°C – 115°C (slcn)	260°C – 324.26°C (Chitosan) 230°C – 340°C (slcn)	50°C - 380°C	20°C/min
[38]	Pure chitosan, gelatine and chitosangelatine nanofibers	85.48°C (pure chitosan) 62.73°C (gelatine) 74.08°C (chitosangelatine)	-	-20°C-100°C	10°C/min
[39]	Chitosan, Erythromycin estolate	~90°C (Chitosan) 165°C (Erythromycin estolate	-	27°C-400°C	10°C/min
[40]	Chitosan	100°C (Chitosan	310°C(Chitosan)	0°C-500°C	5°C/min
[41]	Chitosan	90°C – 108°C (Chitosan) 175°C (Chitosan, after cooling	>230°C (not specified	50°C-550°C,3°C-220°C	20°C/min
[42]	Chitosan and Sodium Alginate	-	(Biofield Treated Chitosan)	24°C-400°C	10°C/min

Figure 4.3 shows the spontaneous DSC results. Endothermic peak points at around 30-45 °C that are related with the evaporation of saturated and bonded water was found to be consistent with the existing literature. Exothermic peak points at around 200 °C are observed which are related with the degradation of chitosan [37-42].

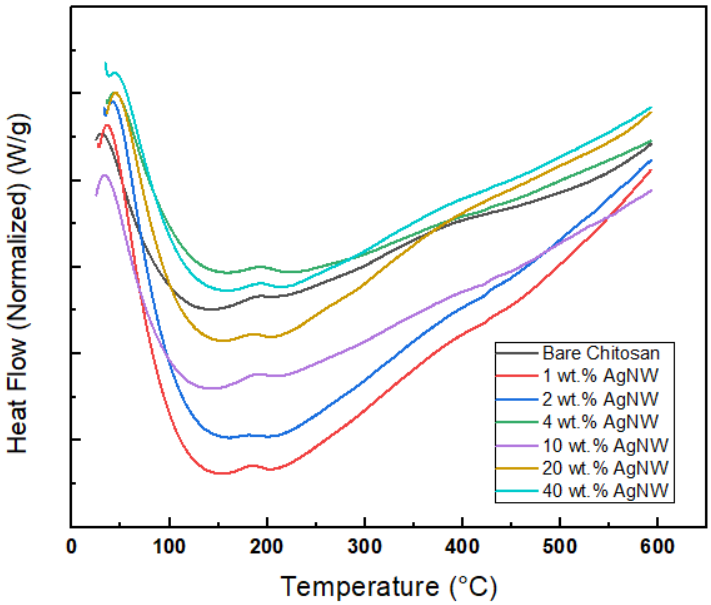

Figure 4.3 Spontaneous DSC measurements results of bare Chitosan, Ag NW/chitosan nanocomposites with Ag NW loadings of (a) 1 wt.%, (b) 2 wt.%, (c) 4 wt.%, (d) 10 wt.%, (e) 20 wt.% and (f) 40 wt.%.

4.2.2. Thermogravimetric Analysis (TGA)

Table 4.2 shows the TGA thermograms of chitosan and Ag NW/ chitosan nanocomposite films. In the literature analyses were conducted with various heat rates such as 20 °C/min, 10 °C/min and 5 °C/min.

Tablo 4.2 Thermal Properties through TGA analysis for chitosan and composite materials in literature.

Ref.	Chitosan used/compared	Decomposition Temperature (Td)*	Mass of sample	Heating Range	Heating Rate
[37]	Chitosan and silver loaded chitosan nanoparticles (slcn)	50°C– 150°C (first stage) 260°C – 365°C (second stage)	5mg	50°C – 500°C	20°C/min
[42]	Chitosan and sodium Alginate	266°C – 350°C	-	24°C – 400°C	5°C/min
[43]	Chitosan composite films	313°C (Chitosan)**	2-3mg	35°C-550°C	10°C/min
[44]	Chitosan	150°C (first stage)	10mg	0°C-500°C	10K/min
[45]	Chitosan	(1,505*B + 369.7)C (second stage)***	5-6 mg	30°C-650°C	10,14,18,22,26, 30 K/min
[46]	Chitosan and Hydroxy Propyle Methyl Cellulose (HPMC) films	303.4°C – 298.9°C – 370.4°C ****	2-6 mg	24°C-600°C	10°C/min
[47]	Chitosan and Chitosan/Agar blended films	50°C – 150°C (first stage) ~210°C (second stage transition	4-10 mg	40°C-500°C	10°C/min
[48]	Chitosan modified by cinnamic acid	220°C (first stage) 295°C – 470°C (second stage)	10 mg	24°C-500°C	10°C/min

Figure 4.4 shows the TGA thermograms of bare chitosan and the Ag NW/ chitosan nanocomposite films with different Ag NW loadings. The results are consistent with the DSC results which recalls the temperatures in spontaneous DSC and TGA analyses. Two stage decomposition is observed consistent with the existing literature.[17,42-48]

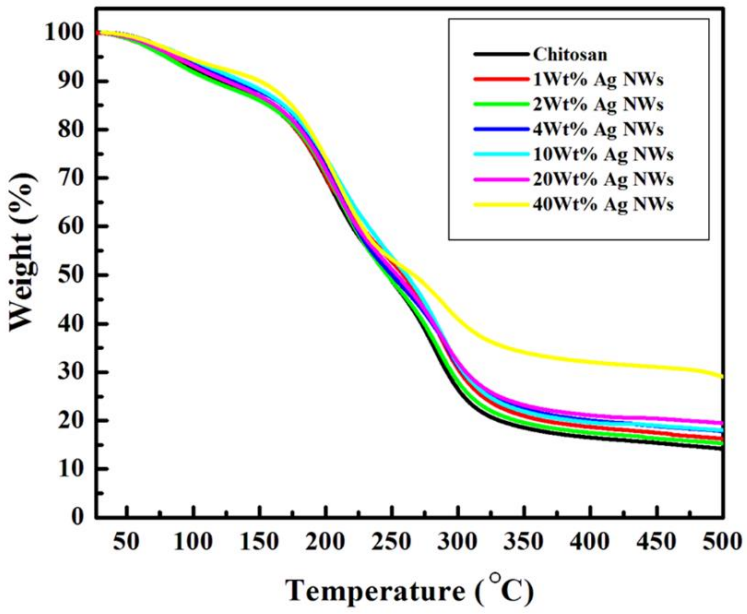

Figure 4.4 TGA thermograms for of bare chitosan, Ag NW/ chitosan nanocomposites with Ag NW loadings of (a) 1 wt. %, (b) 2 wt. %, (c) 4 wt. %, (d) 10 wt. %, (e) 20 wt. % and (f) 40 wt. %.

Degradation temperatures shifted to higher temperatures and the degradation behavior trend is similar when it is compared. Also, degradation temperature around 140 °C - 220 °C and 260 °C - 290 °C observed.

4.3. Conductivity Test Results

Figure 4.5 shows the conductivity measurement results for bare chitosan and Ag NW/ chitosan nanocomposites with different Ag NW loadings. While bare chitosan has an electrical conductivity value of 10^{-5} S/m, Ag NW/ chitosan nanocomposite films have electrical conductivity values of $4x10^{-4}$ S/m, 10^{-2} S/m, and 10^{-1} S/m for 12.5 wt. %, 25 wt. % and 50 wt. % Ag NW loadings, respectively. As can be seen from Figure 4.5, the conductivity values increase with increasing Ag NW loading within the nanocomposites.

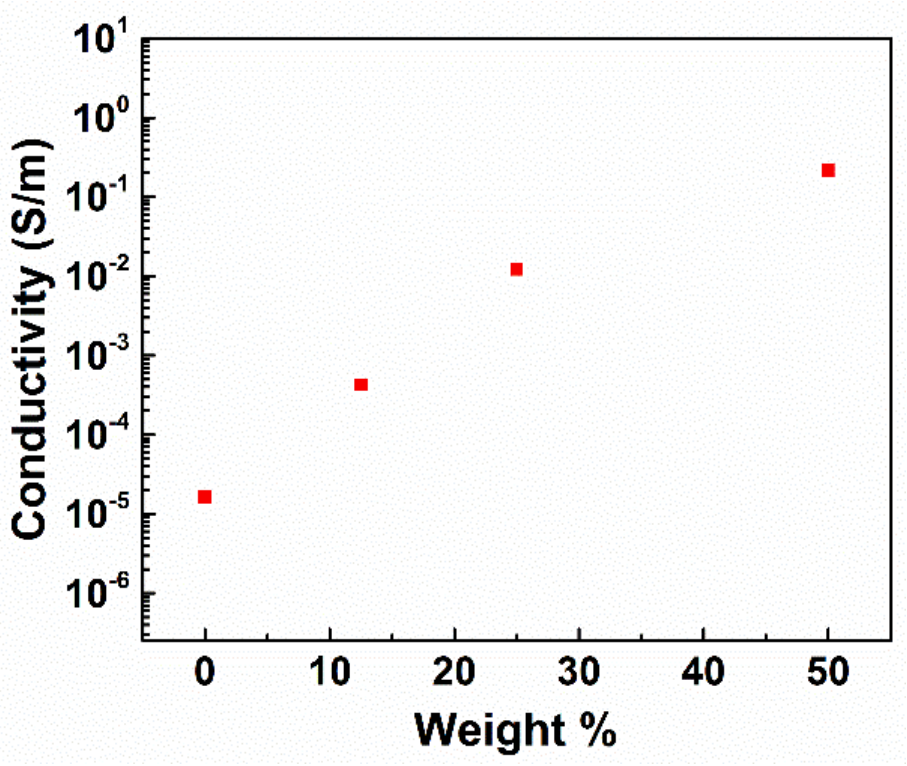

Figure 4.5 Conductivity values for different concentrations of Ag NW/chitosan nanocomposite films with different Ag NW loadings.

4.4. Antibacterial Tests

4.4.1. Disk Diffusion Tests

Disk diffusion test results show the inhibition zones provided by samples against different types of bacteria. It can be seen from the Figure 4.6 that chitosan itself provides an inhibition zone with a diameter of around 8 mm, exhibiting antibacterial properties. The main reason for this fact is the antimicrobial property of chitosan.

The antibacterial mechanism of chitosan and its derivatives is not known. However, it is stated that a polycationic structure is a prerequisite for antibacterial activity. Unlike chitin, chitosan and chitosan oligosaccharides contain free amino groups in their structure. When the pH of the medium is lower than the pKa (6.3-6.5) of the amino groups of chitosan and its derivatives, chitosan and its derivatives gain a polycationic structure. The main role in antibacterial activity has been reported to be played by the electrostatic interaction between chitosan in polycationic form and anionic components present on the surface of microorganisms (eg lipopolysaccharides and cell surface proteins in Gram-negative bacteria) [2]. As a result of electrostatic interaction, the distribution of negative and positive charges on the cell surface is differentiated and thus membrane stability is impaired and permeability is changed. As the permeability of the membrane changes, nutrients cannot enter the cell or their intracellular components leak out of the cell, causing cell death [18, 25, 26].

In Figure 4.6 (a), (b) and (c), the inhibition zones of Ag NW/ chitosan nanocomposite films with different Ag NW loadings against *S.Aureus* and *E.Coli* are shown. One can summarize that the antibacterial activity increases with NW loading, which is expected and consistent with the existing literature. However, the enhancement in the antibacterial activity was not found to be proportional to the Ag NW amount.

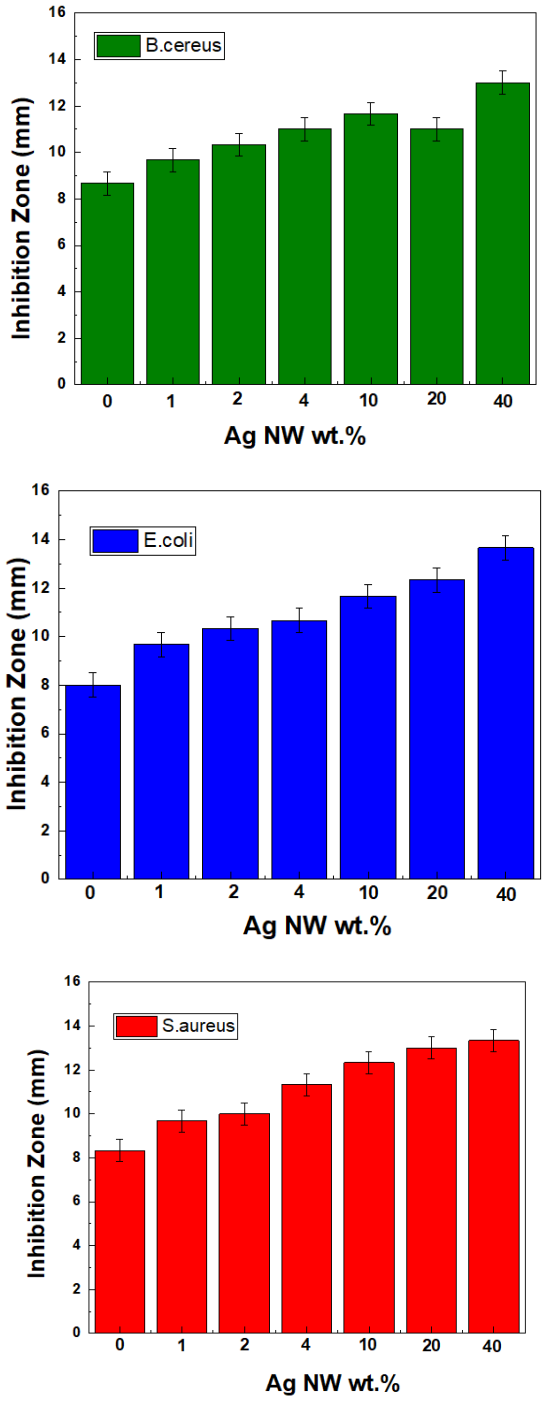

Figure 4.6 Disk diffusion test results and inhibition zone diameters against S. Aureus B. cereus and E.Coli species for bare chitosan and Ag NW/chitosan nanocomposite films with varying Ag NW loadings.

The main reason for this fact can be the wrinkles that forms within the composites in the agar plate, which decreases the performance of nanocomposites. The other reason would be the changes in ionic strength of the medium, which might affect the inhibitory activity of chitosan [39]. The increase in the concentration of metal ions, especially, decreases the chelating capacity of chitosan, thus reducing its antibacterial activity [23, 24]. In addition, since cations present in the environment will compete with polycationic chitosan to bind to negative charges in the bacterial cell wall, they may cause a decrease in antimicrobial activity [2].

4.5. ECG MEASUREMENTS

4.5.1. Skin Electrode Impedance

Skin–electrode touch impedance is important in biopotential recordings as it influences the transmitted signal at the amplifier interface [61]. The effect is similar to the filtering of the body's actual biopotentials [62]. Figure 4.7 shows equivalent circuit impedance. It is highly important to have equal Z_1 and Z_2 values so that the measurements would yield more accurate results. Electrodes should have homogeneous and identical properties and skin electrode impedance should have a low value as much as possible. One reason for the poor quality of dry electrodes is the higher impedance values when compared with the standard wet electrodes.

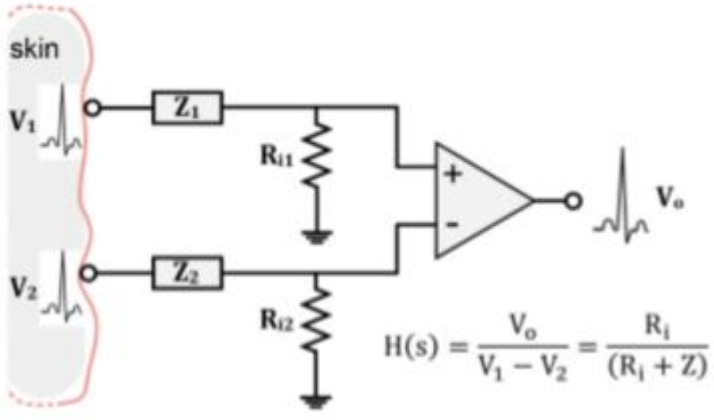

Figure 4.7 Equivalent circuit for the skin–electrode impedance [adapted from 57].

4.5.2. Wet Electrode and Dry Composite Electrode Circuit Model

Figure 4.8 shows the skin-electrode interface analogous circuit that begins with a half-cell electrode potential followed by the electrode-electrolyte interface between the electrode and the liquid. This is characterized by a capacitance due to electrical double-layer structure Cd and transition resistance Rd charging. A sequence resistance Rs is the template of the gel medium [61]. In this work, upon increasing the Ag NW loading in Ag NW/ chitosan nanocomposite films, the resistance of the electrodes decreased, which resulted in a decrease in the impedance value. This eventually enhances the signal quality.

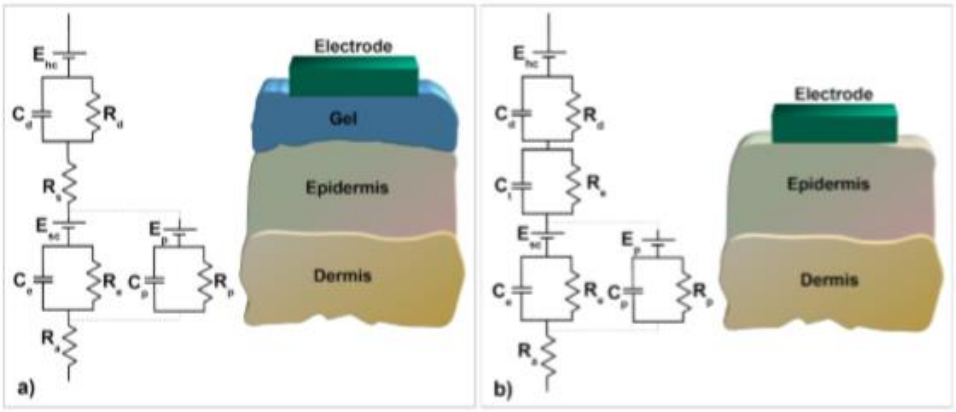

Figure 4.8 *Equivalent circuit for skin–electrode interface for (a) a traditional wet electrode and (b) a dry electrode [adapted from 57].*

ECG measurements were conducted with 4 electrodes and their locations are shown in Chapter 3. Measurements were taken with 6 channels which were 1,2,3 “aVR”, ”aVL” , ” aVF”, respectively. ECG measurement results for pure chitosan electrode, Ag NW/ chitosan nanocomposite electrodes with a Ag NW loading of 4 wt. % and 20 wt. % are shown, in Figures 4.9, 4.10, and 4.11, respectively. Note that all results were filtered with 3 electronic filters that were low pass filters, high pass filters, and line interference filters. All of which dramatically enhanced the performance of the electrodes. As can be seen from Figure 4.9 with bare chitosan dry electrode, without

Ag NWs, the user was unable to read useful signals and electrode failed on its mission. However, upon the use of Ag NW/ chitosan nanocomposites even with a Ag NW loading of 4 wt. % , P, QRS, T waves were found to appear (Figure 4.10). With a further increase in the Ag NW loading to 20 wt. %, electrode performance got dramatically improved without the use of a gel (Figure 4.11).

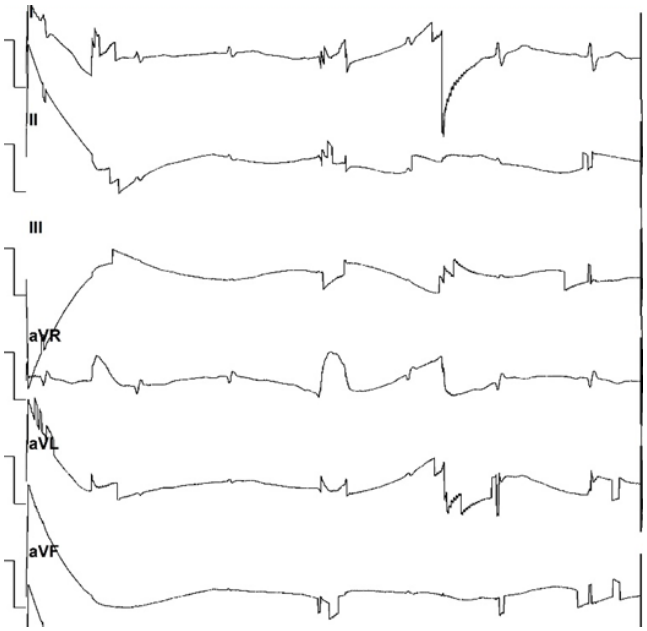

Figure 4.9 ECG measurement results which were taken with 6 channels of bare chitosan electrodes.

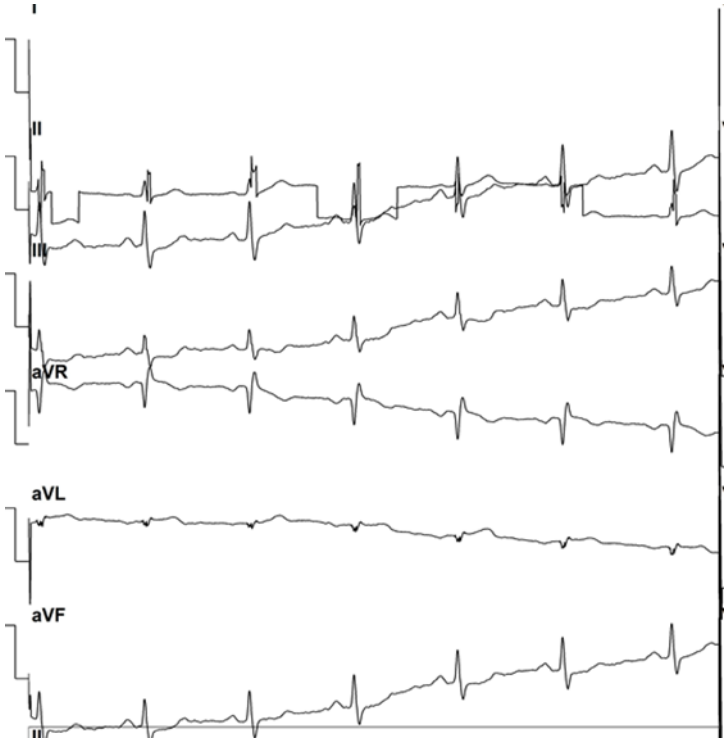

Figure 4.10 ECG measurement results which were taken with 6 channels of 4 wt. % Ag NW/chitosan nano composite electrodes.

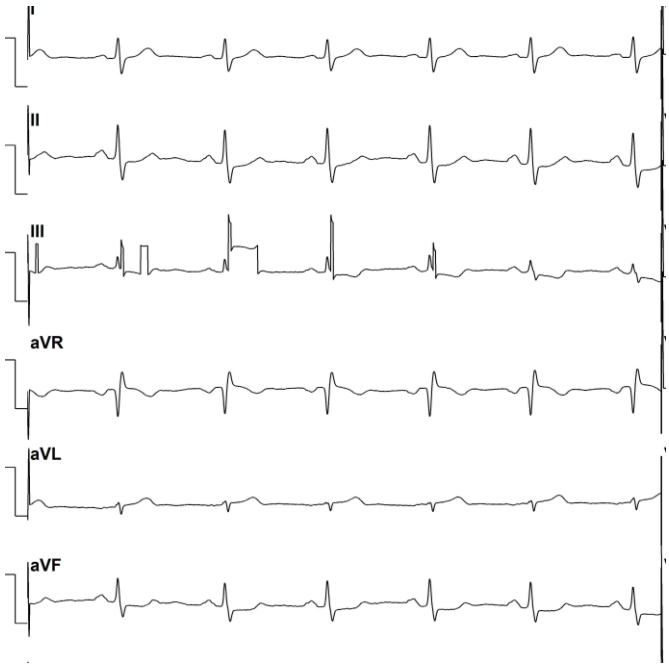

Figure 4.11 ECG measurement results which were taken with 6 channels of 20 wt. % Ag NW/chitosan nanocomposite electrodes.

Finally a Ag NW loading of 33 wt. % was used as a dry electrode and ECG measurement results are provided in Figure 4.12. It can be seen that the signal quality improved a lot, which was expected because the conductivity of the nanocomposites increases with the Ag NW loading.

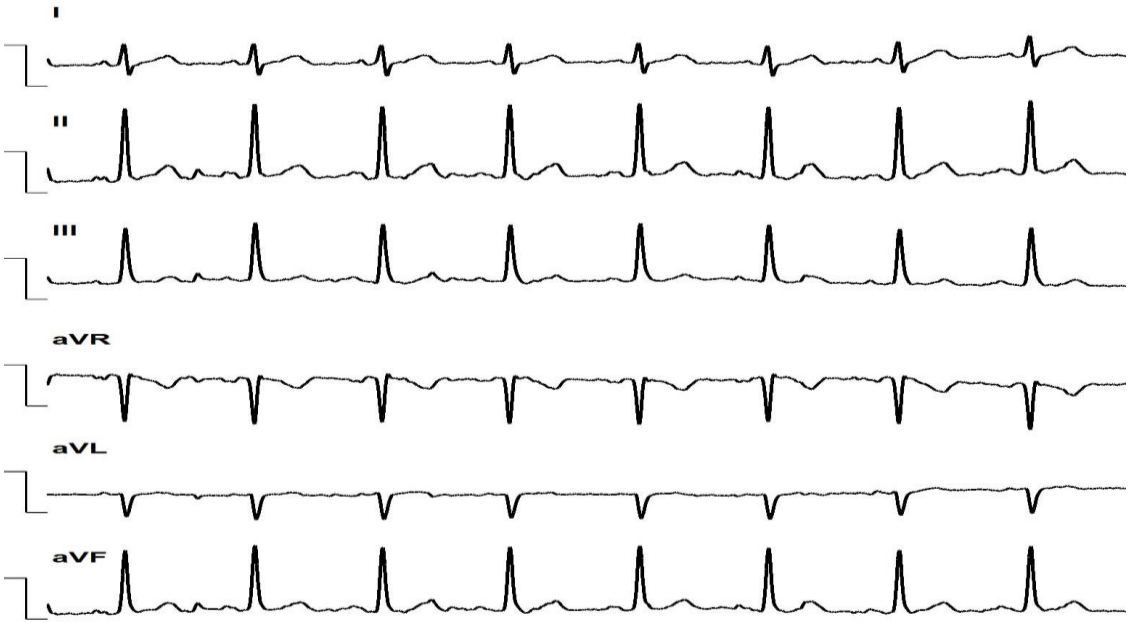

Figure 4.12 ECG measurement results which were taken with 6 channels of 33 wt. % Ag NW/chitosan nanocomposite electrodes.

To make a comparison, four standard gel electrodes were used in the same location and the ECG measurement results are provided in Figure 4.13. The results were found to be similar to those obtained using Ag NW/ chitosan nanocomposite electrodes with a Ag NW loading of 33 wt. %.

Considering that the polymer electrode is highly elastic, fabricated Ag NW/ chitosan nanocomposite electrodes with promising ECG performance are good candidates for wearable electrodes with long term stability.

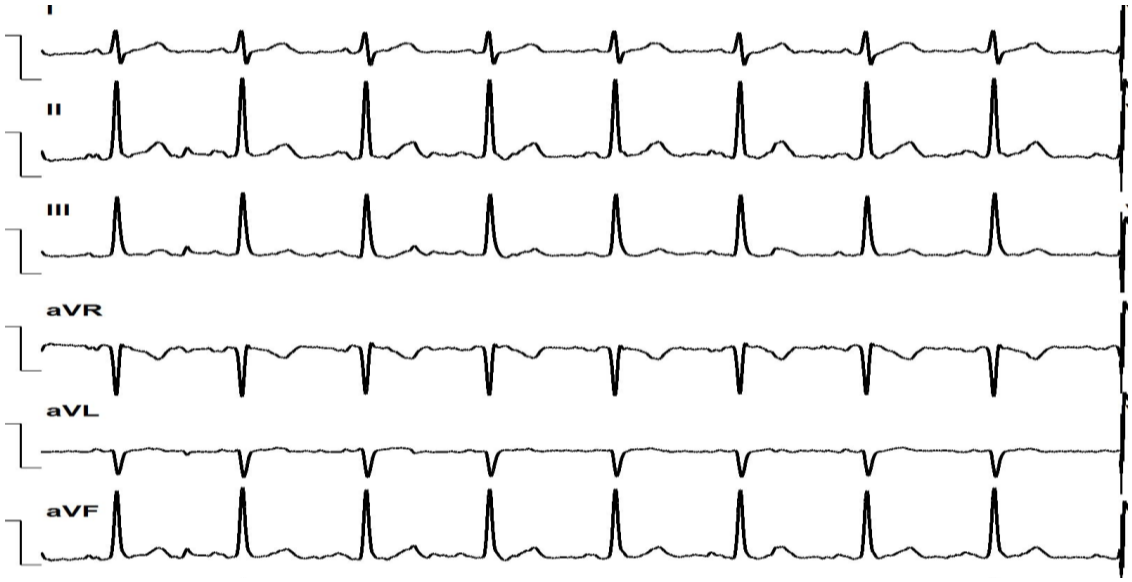

Figure 4.13 *ECG measurement results of standard wet electrodes.*

CHAPTER 5

CONCLUSIONS AND FUTURE RECOMMENDATIONS

5.1. Conclusions

In this thesis, nanocomposites were fabricated using Ag NWs as a filler and chitosan as a bio-polymer matrix. Electrical and thermal characterization of the nanocomposites were conducted. The effect of the Ag NW loading on the antimicrobial effects, electrical resistance, and thermal properties of chitosan-based nanocomposites were determined. Ag NW/ chitosan nanocomposite electrodes were fabricated using solvent casting method. A parametric study was conducted with different Ag NW loadings of ranging from 1 to 40 wt. %. Finally, the fabricated ECG electrodes were tested in-vitro.

ECG measurements with the utilization of fabricated nanocomposites as dry electrodes were conducted. It was determined that even small amounts of Ag NW loading (such as 4 wt. %) makes the ECG signals identifiable and useful for the operator. The quality of the signals got improved proportionally with increasing Ag NW loading. Upon considering the potential medical applications of the fabricated ECG electrodes, antibacterial activity is a required and useful improvement.

It is observed from the study that its antibacterial properties of chitosan got improved by the addition of Ag NWs and an inhibition zone diameter up to 15 mm was obtained for the nanocomposite samples. Moreover, this study revealed that the developed composites have a potential to be used in ECG measurements as a dry electrode, which would certainly enable timely intervention upon a change in the health status of the monitored patients. These dry and flexible electrodes can also enable the realization of wearable ECG sensors for life-long measurements if needed.

5.1.1. Future Recommendations

As a future work, different molecular weights of chitosan can be employed to better understand its effect on antibacterial, electrical and thermal behavior of the fabricated nanocomposites.

In addition, as an ECG electrode the motion artifacts can be cleaned out. As a wearable electrode, long-term use, stability and cleaning issues can be further investigated. Moreover, both conductivity and impedance response of the ECG electrodes and composite films under different pressure and temperature conditions can be investigated. Furthermore, the effect of other antibacterial tests such as time kill assay and adhesion test can be conducted to better understand its limits under aging and Ag NW's impact on the antibacterial property.

In terms of characterization, impedance spectroscopy analysis can be used to investigate the behavior of the electrodes.

Last but not least, this study can be extended not only to ECG but also to other biopotential signal tracking instruments such as electroencephalogram (EEG) or electromyography (EMG) devices.

REFERENCES

[1] R. A. A. Muzzarelli, J. Boudrant, D. Meyer, N. Manno, M. DeMarchis, and M. G. Paoletti, "Current views on fungal chitin/chitosan, human chitinases, food preservation, glucans, pectins and inulin: A tribute to Henri Braconnot, precursor of the carbohydrate polymers science, on the chitin bicentennial", Carbohydrate Polymers, vol. 87, no. 2, pp. 995–1012, 2012.

[2] M. Kong, X. G. Chen, K. Xing, and H. J. Park, "Antimicrobial properties of chitosan and mode of action: A state of the art review", International Journal of Food Microbiology, vol. 144, no. 1, pp. 51–63, 2010.

[3] K. V. H. Prashanth and R. N. Tharanathan, "Chitin/Chitosan: Modifications and Their Unlimited Application Potential—An Overview", Trends in Food Science & Technology, vol. 18, No.3, pp. 117-131, 2007.

[4] I. Younes and M. Rinaudo, "Chitin and chitosan preparation from marine sources. Structure, properties and applications", Mar Drugs, vol. 13, no. 3, pp. 1133–1174, 2015.

[5] C. Marambio- Jones and E. Hoek, "A Review of the Antibacterial Effects of Silver Nanomaterials and Potential Implications for Human Health and the Environment", Journal of Nanoparticle Research, vol. 12,no.1, pp. 1531–1551, 2010.

[6] C.-Y. Chen and C.-L. Chiang, "Preparation of cotton fibers with antibacterial silver nanoparticles", Materials Letters, vol. 62, no. 21, pp. 3607–3609, 2008.

[7] L. Liu, C. He, J. Li, J. Guo, D. Yang, and J. Wei, "Green synthesis of silver nanowires via ultraviolet irradiation catalyzed by phosphomolybdic acid and their antibacterial properties", New J. Chem., vol. 37, no. 7, pp. 2179–2185, 2013.

[8] Y. Chen, W.Lan, J. Wang, R. Zhu, Z. Yang, D.Ding, G. Tang, K. Wang, Q. Su, E.Xie, “Highly flexible, transparent, conductive and antibacterial films made of spin-coated silver nanowires and a protective ZnO layer”, Physica E: Low-dimensional Systems and Nanostructures, vol. 76, pp. 88–94, 2016.

[9] P. Giesz, E. Mackiewicz, A. Nejman, G. Celichowski, and M. Cieślak, “Investigation on functionalization of cotton and viscose fabrics with AgNWs”, Cellulose, vol. 24, no. 1, pp. 409–422, 2017.

[10] S. Jiang and C. P. Teng, “Fabrication of silver nanowires-loaded polydimethylsiloxane film with antimicrobial activities and cell compatibility”, Materials Science and Engineering: C, vol. 70, pp. 1011–1017, 2017.

[11] W. Xie, P. Xu, and Q. Liu, “Antioxidant activity of water-soluble chitosan derivatives”, Bioorganic & Medicinal Chemistry Letters, vol. 11, no. 13, pp. 1699–1701, 2001.

[12] M. Dash, F. Chiellini, R. M. Ottenbrite, and E. Chiellini, “Chitosan—A versatile semi-synthetic polymer in biomedical applications”, Progress in Polymer Science, vol. 36, no. 8, pp. 981–1014, 2011.

[13] R. Jayakumar, D. Menon, K. Manzoor, S. V. Nair, and H. Tamura, “Biomedical applications of chitin and chitosan based nanomaterials—A short review”, Carbohydrate Polymers, vol. 82, no. 2, pp. 227–232, 2010.

[14] K. Kurita, “Chitin and Chitosan: Functional Biopolymers from Marine Crustaceans”, Marine Biotechnology, vol. 8, no. 3, p. 203, 2006.

[15] R. C. Goy, D. De Britto, and O. B. G. Assis, “A review of the antimicrobial activity of chitosan”, Polimeros, vol.19, no.3, pp.241-247, 2009.

[16] M. N. . Ravi Kumar, “A review of chitin and chitosan applications”, Reactive and Functional Polymers, vol. 46, no. 1, pp. 1–27, 2000.

[17] X. F. Guo, K. Kikuchi, Y. Matahira, K. Sakai, and K. Ogawa, “Water-Soluble Chitin of Low Degree Of Deacetylation”, Journal of Carbohydrate Chemistry, vol. 21, no. 1–2, pp. 149–161, 2002.

[18] S. V. Nemtsev, A. I. Gamzazade, S. V. Rogozhin, V. M. Bykova, and V. P. Bykov, “Deacetylation of Chitin under Homogeneous Conditions”, Applied Biochemistry and Microbiology, vol. 38, no. 6, pp. 521–526, 2002.

[19] H. K. No, S. H. Kim, S. H. Lee, N. Y. Park, and W. Prinyawiwatkul, “Stability and antibacterial activity of chitosan solutions affected by storage temperature and time”, Carbohydrate Polymers, vol. 65, no. 2, pp. 174–178, 2006.

[20] P. Dutta, J. Dutta, and V. Tripathi, “Chitin and chitosan: Chemistry, properties and applications”, J Sci Indus Res, vol. 63, no. 1, 2003.

[21] J. D. Funkhouser and N. N. Aronson, “Chitinase family GH18: evolutionary insights from the genomic history of a diverse protein family”, BMC Evolutionary Biology, vol. 7, no. 1, p. 96, 2007.

[22] Y. M. Yang, W. Hu, X. D. Wang, and X. S. Gu, “The controlling biodegradation of chitosan fibers by N-acetylation in vitro and in vivo”, Journal of Materials Science: Materials in Medicine, vol. 18, no. 11, pp. 2117–2121, 2007.

[23] E. I. Rabea, M. E.-T. Badawy, C. V. Stevens, G. Smagghe, and W. Steurbaut, “Chitosan as Antimicrobial Agent: Applications and Mode of Action”, Biomacromolecules, vol. 4, no. 6, pp. 1457–1465, 2003.

[24] H. K. No, S. P. Meyers, W. Prinyawiwatkul, and Z. Xu, “Applications of Chitosan for Improvement of Quality and Shelf Life of Foods: A Review”, Journal of Food Science, vol. 72, no. 5, pp. R87–R100, 2007.

[25] Z. Guo, R. Xing, S. Liu, Z. Zhong, X. Ji, L. Wang, P. Li, “Antifungal properties of Schiff bases of chitosan, N-substituted chitosan and quaternized chitosan”, Carbohydrate Research, vol. 342, no. 10, pp. 1329–1332, 2007.

[26] Z. Guo, R. Xing, S. Liu, Z. Zhong, X. Ji, L. Wang, P. Li, "The influence of molecular weight of quaternized chitosan on antifungal activity", Carbohydrate Polymers, vol. 71, no. 4, pp. 694–697, 2008.

[27] C. Nataraj, A. Jalali ve P. Ghorbanian, «ResearchGate,» [Çevrimiçi]. Available: https://www.researchgate.net/figure/The-components-of-the-ECG-signal_fig1_224830806.

[28] V. Marozas, A. Petrenas, S. Daukantas, and A. Lukosevicius, "A comparison of conductive textile-based and silver/silver chloride gel electrodes in exercise electrocardiogram recordings", Journal of Electrocardiology, vol. 44, no. 2, pp. 189–194, 2011.

[29] B. Liu, Z. Luo, W. Zhang, Q. Tu, and X. Jin, "Silver nanowire-composite electrodes for long-term electrocardiogram measurements", Sensors and Actuators A: Physical, vol. 247, pp. 459–464, 2016.

[30] G.-W. Huang, H.-M. Xiao, and S.-Y. Fu, "Wearable Electronics of Silver-Nanowire/Poly(dimethylsiloxane) Nanocomposite for Smart Clothing", Scientific Reports, vol. 5, no. 1, p. 13971, 2015.

[31] A. C. Myers, H. Huang, and Y. Zhu, "Wearable silver nanowire dry electrodes for electrophysiological sensing", RSC Adv., vol. 5, no. 15, pp. 11627–11632, 2015.

[32] M. Weder, D. Hegemann, M. Amberg, M. Hess, L. Boesel, R. Abächerli, V. Meyer, and R. Rossi, "Embroidered Electrode with Silver/Titanium Coating for Long-Term ECG Monitoring", Sensors, vol. 15, no. 1, pp. 1750–1759, 2015.

[33] B. Liu, H. Tang, Z. Luo, W. Zhang, Q. Tu, and X. Jin, "Wearable carbon nanotubes-based polymer electrodes for ambulatory electrocardiographic measurements", Sensors and Actuators A: Physical, vol. 265, 2017.

[34] S. Seyedin, P. Zhang, M. Naebe, S. Qin, J. Chen, X. Wang, J.M. Razal, “Textile strain sensors: a review of the fabrication technologies, performance evaluation and applications”, Mater. Horiz., vol. 6, no. 2, pp. 219–249, 2019.

[35] P. G. Whitten, A. A. Gestos, G. M. Spinks, K. J. Gilmore, and G. G. Wallace, “Free standing carbon nanotube composite bio-electrodes”, Journal of Biomedical Materials Research Part B: Applied Biomaterials, vol. 82B, no. 1, pp. 37–43, Jul. 2007.

[36] Y. Song, P.Li, M.Li, H.Li, C.Li, D.Sun, B.Yang, “Fabrication of chitosan/Au-TiO2 nanotube-based dry electrodes for electroencephalography recording”, Materials Science and Engineering: C, vol. 79, pp. 740–747, 2017.

[37] W. Ali, S. Rajendran, and M. Joshi, “Synthesis and characterization of chitosan and silver loaded chitosan nanoparticles for bioactive polyester”, Carbohydrate Polymers, vol. 83, pp. 438–446, 2011.

[38] B. Dhandayuthapani, U. M. Krishnan, and S. Sethuraman, “Fabrication and characterization of chitosan-gelatin blend nanofibers for skin tissue engineering”, Journal of Biomedical Materials Research Part B: Applied Biomaterials, vol. 94B, no. 1, pp. 264–272, 2010.

[39] P. Shende, S. Kumar Yadava, and P. S. Patil, “Development and Characterization of Chitosan Nanoparticles Containing Erthromycin Estolate”, International Journal of Pharmaceutical Applications, vol. 5, no.1, pp. 1-7, 2014.

[40] J. M. Nieto, C. Peniche-Covas, and G. Padro´n, “Characterization of chitosan by pyrolysis-mass spectrometry, thermal analysis and differential scanning calorimetry”, Thermochimica Acta, vol. 176, pp. 63–68, 1991.

[41] F. S. Kittur, K. V. Harish Prashanth, K. Udaya Sankar, and R. N. Tharanathan, “Characterization of chitin, chitosan and their carboxymethyl derivatives by differential scanning calorimetry”, Carbohydrate Polymers, vol. 49, no. 2, pp. 185–193, 2002.

[42] S. Jana, M. Kumar Trivedi, and R. M. Tallapragada, “Characterization of Physicochemical and Thermal Properties of Chitosan and Sodium Alginate after Biofield Treatment”, Pharmaceutica Analytica Acta, vol. 6, 2015.

[43] G. Cardenas and S. Miranda, “FTIR and TGA studies of chitosan composite films”, J. Chil.Chem. Soc, vol. 49, pp. 291–295, 2004.

[44] P. Dhawade and R. N. Jagtap, “Characterization of the glass transition temperature of chitosan and its oligomers by temperature modulated differential scanning calorimetry”, Adv Appl Sci Res, vol. 3, pp. 1372–1382, 2012.

[45] P.-Z. Hong, S.-D. Li, C.-Y. Ou, C.-P. Li, L. Yang, and C.-H. Zhang, “Thermogravimetric analysis of chitosan”, Journal of Applied Polymer Science, vol. 105, no. 2, pp. 547–551, 2007.

[46] J. Rotta, E. Minatti, and P. L. M. Barreto, “Determination of structural and mechanical properties, diffractometry, and thermal analysis of chitosan and hydroxypropylmethylcellulose (HPMC) films plasticized with sorbitol”, Food Science and Technology, vol. 31, pp. 450 – 455, 2011.

[47] E. A. Elhefian, M. M. Nasef, and A. H. Yahaya, “Preparation and Characterization of Chitosan/Agar Blended Films: Part 2. Thermal, Mechanical, and Surface Properties”, E-Journal of Chemistry, vol. 9, p. 285318, 1900.

[48] J. Zhou, X. Xu, H. Yu, and G. Lubineau, “Deformable and wearable carbon nanotube microwire-based sensors for ultrasensitive monitoring of strain, pressure and torsion”, Nanoscale, vol. 9, no. 2, pp. 604–612, 2017.

[49] M.-C. Choi, Y. Kim, and C.-S. Ha, “Polymers for flexible displays: From material selection to device applications”, Progress in Polymer Science, vol. 33, no. 6, pp. 581–630, 2008.

[50] C.-L. Huang, L.-J. Bao, P. Luo, Z.-Y. Wang, S.-M. Li, and E. Y. Zeng, “Potential health risk for residents around a typical e-waste recycling zone via inhalation of size-fractionated particle-bound heavy metals”, Journal of Hazardous Materials, vol. 317, pp. 449–456, 2016.

[51] R. S. Kohlman, D. B. Tanner, G. G. Ihas, Y. G. Min, A. G. MacDiarmid, and A. J. Epstein, “Inhomogeneous Insulator-Metal Transition in Conducting Polymers” ,Synthetic Metals, vol. 84, no. 1, pp. 709–714, 1997.

[52] L.-X. Wang, X.-G. Li, and Y.-L. Yang, “Preparation, properties and applications of polypyrroles”, Reactive and Functional Polymers, vol. 47, no. 2, pp. 125–139, 2001.

[53] P. M. George, A. W. Lyckman, D. A. LaVan, A.Hegde, Y.Leung, R. Avasare, C.Testa, P.M. Alexander, R. Langer, M. Sur, “Fabrication and biocompatibility of polypyrrole implants suitable for neural prosthetics”, Biomaterials, vol. 26, no. 17, pp. 3511–3519, 2005.

[54] X. Cui, J. Wiler, M. Dzaman, R. A. Altschuler, and D. C. Martin, “In vivo studies of polypyrrole/peptide coated neural probes”, Biomaterials, vol. 24, no. 5, pp. 777–787, 2003.

[55] F. Gao, N. Zhang, X. Fang, and M. Ma, “Bioinspired Design of Strong, Tough, and Highly Conductive Polyol-Polypyrrole Composites for Flexible Electronics”, ACS Appl. Mater. Interfaces, vol. 9, no. 7, pp. 5692–5698, 2017.

[56] J. Ouyang and Y. Li, “Preparation and characterization of flexible polypyrrole nitrate films”, Synthetic Metals, vol. 79, no. 2, pp. 121–125, 1996.

[57] M. Mehrali, S. Bagherifard, M. Akbari, A.Thakur, B. Mirani, M. Mehrali, M. Hasany, G. Orive, P. Das, J. Emneus, T.L. Andresen, A. Dolatshahi-Pirouz, "Blending Electronics with the Human Body: A Pathway toward a Cybernetic Future", Advanced Science, vol. 5, no. 10, p. 1700931, 2018.

[58] A. Leal-Egaña and T. Scheibel, "Silk-based materials for biomedical applications", Biotechnology and Applied Biochemistry, vol. 55, no. 3, pp. 155–167, 2010.

[59] S. Coskun, B. Aksoy, and H. E. Unalan, "Polyol Synthesis of Silver Nanowires: An Extensive Parametric Study", Crystal Growth & Design, vol. 11, no. 11, pp. 4963–4969, 2011.

[60] F.Zhang, Q.Lu, X.Yue, B. Zuo, M.Qin, F.Li, D. L.Kaplan, X. Zhang, "Regeneration of high-quality silk fibroin fiber by wet spinning from CaCl2–formic acid solvent", Acta Biomaterialia, vol. 12, pp. 139–145, 2015.

[61] N. Watanabe, S. Isobe, T. Okumura, H. Mori, T. Yamada, K. Nishimura, M. Miura, S. Sakai, T. Murohara, "Relationship between QRS score and microvascular obstruction after acute anterior myocardial infarction", Journal of Cardiology, vol. 67, no. 4, pp. 321–326, 2016.

[62] K. Day, I. Oliva, E. Krupinski, and F. Marcus, "Identification of 4th intercostal space using sternal notch to xiphoid length for accurate electrocardiogram lead placement", Journal of electrocardiology, vol. 48, no. 6, pp. 1058–1061, 2015.